



**HAL**  
open science

## Effect of temperature on the mechanical properties of fine-grained soils - A review

Md Azhar, Somenath Mondal, Anh Minh A.M. Tang, Akhileshwar Singh

► **To cite this version:**

Md Azhar, Somenath Mondal, Anh Minh A.M. Tang, Akhileshwar Singh. Effect of temperature on the mechanical properties of fine-grained soils - A review. *Geothermics*, 2024, 116 (12), pp.102863. 10.1016/j.geothermics.2023.102863 . hal-04374980

**HAL Id: hal-04374980**

**<https://enpc.hal.science/hal-04374980>**

Submitted on 22 Jul 2024

**HAL** is a multi-disciplinary open access archive for the deposit and dissemination of scientific research documents, whether they are published or not. The documents may come from teaching and research institutions in France or abroad, or from public or private research centers.

L'archive ouverte pluridisciplinaire **HAL**, est destinée au dépôt et à la diffusion de documents scientifiques de niveau recherche, publiés ou non, émanant des établissements d'enseignement et de recherche français ou étrangers, des laboratoires publics ou privés.



24 **ABSTRACT:** Contemporary geotechnical engineering practice encompasses design and  
25 construction of thermo-active geo-structures or structures which would encounter thermal  
26 cycles throughout its service life. Therefore, understanding the effect of temperature on soil  
27 mechanical properties becomes inevitable. Being a complex and coupled phenomenon it has  
28 been quite challenging for the researchers to study experimentally and theoretically the  
29 thermo-mechanical behaviour of fine-grained soil. Nonetheless, there are numerous studies  
30 which contribute significantly to gain insight about thermo-mechanical behaviour of soils.  
31 Incidentally, till date, on this arena of research, no comprehensive review, which provides a  
32 holistic development of the subject and its connection with the field application, is available.  
33 The prime objective of the present study is to critically appraise the state-of-the-art  
34 understanding on thermo-mechanical behaviour of fine-grained soils through a  
35 comprehensive literature review. Moreover, this paper also describes the concept of thermo-  
36 elasto-plastic strain and thermal creep behaviour of fine-grained soils.

37

38 **Keywords:** Fine-grained soils, Temperature-induced volumetric deformation, Mechanisms,  
39 Thermo-elasto-plastic behaviour.

40

41

42

43

44

45

46

47

48

## 49 **1. Introduction**

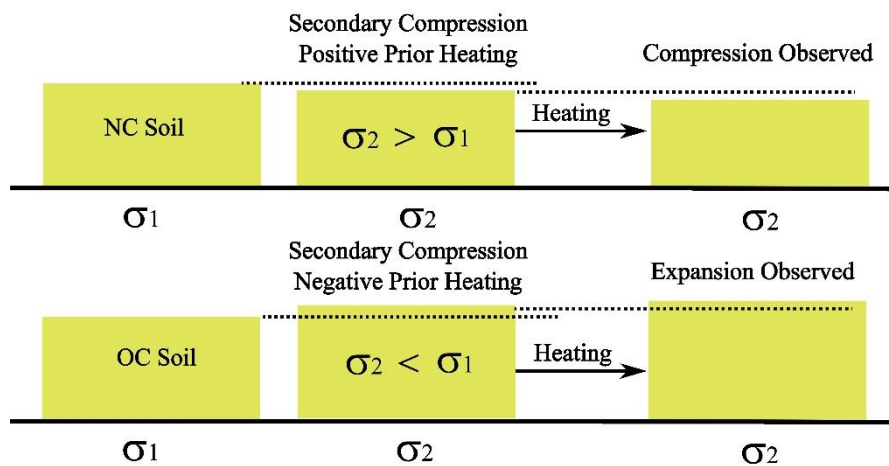
50           Understanding the thermo-mechanical behaviour of fine-grained soils has been  
51 indispensable in modern-day geotechnical engineering practices. This behaviour significantly  
52 influences the overall long-term behaviour of the fine-grained soil upon application of  
53 simultaneous temperature cycles and mechanical loading. In this context, there are numerous  
54 investigations conducted to identify the thermal response of diverse geo-materials. Among  
55 these, a major portion contribute to understand the effect of temperature on volumetric  
56 change (Campanella and Mitchell, 1968; Viridi and Keedwell, 1988) and strength parameters  
57 of soil (Cekerevac and Laloui, 2004; Yavari et al., 2016; Maghsoodi et al., 2020, 2021). In  
58 this regard, most of the investigations have been carried out for the projects related to the  
59 radioactive waste disposal facilities (Viridi and Keedwell, 1988; Rao and Singh, 1999;  
60 Krishnaiah and Singh, 2004a, 2004b; Naidu and Singh, 2004; Sreedeeep et al., 2005; Ojovan  
61 et al., 2019), underground crude oil storage tanks (Padmakumar, 2013), oil-carrying pipelines  
62 ( Brandon and Mitchell, 1989; Manthena and Singh, 2001; Abuel-Naga et al., 2008; Lee et  
63 al., 2010), air-conditioning ducts (Kadali et al., 2013), buried conduits and high voltage  
64 electrical cables (Abuel-Naga et al., 2008; De Moel et al., 2010; Vega and McCartney, 2014),  
65 geothermal energy piles (Di et al., 2000; Bozis et al., 2011), elevated temperature landfills  
66 (McCartney et al., 2019), furnaces, boiler units, forging units, brick kilns and rocket-  
67 launching pads (Kadali et al., 2013). These studies generally analysed the volumetric change  
68 of soil when temperature varies in the range between 0 and 100 °C.

69           This study mainly focuses on the thermo-mechanical behaviour of fine-grained soil, in  
70 which variation of temperature lies between 0 and 100 °C. Therefore, the phase change of  
71 pore water due to variation of temperature has not been induced. For this reason, several  
72 other phenomena of temperature-soil interaction such as soil water freezing/thawing or

73 evaporation, soil mineral alteration due to fire, phase change of soil due to volcanic eruption,  
74 *etc.* are not considered.

75         The thermo-mechanical behaviour of fine-grained soil has been analysed against  
76 application of varying temperature by many researchers in saturated soil (Campanella and  
77 Mitchell, 1968; Demars and Charles, 1982; Hueckel and Baldi, 1990; Burghignoli et al.,  
78 2000; Sultan et al., 2002; Cekerevac and Laloui, 2004; Abuel-Naga et al., 2008; Coccia and  
79 McCartney, 2012; Vega and McCartney, 2014) and unsaturated soil (Romero et al., 2005;  
80 Tang et al., 2008; Uchaipichat and Khalili, 2009; Alsherif and McCartney, 2015; Coccia and  
81 McCartney, 2016a, 2016b). Saturated soil will tend to change its volume in response to the  
82 thermal solicitation when it is heated. Hence this phenomenon is termed as thermal  
83 volumetric change. This process is defined as thermal consolidation if dissipation of pore  
84 water takes place. During undrained condition, the different coefficient of thermal expansions  
85 of soil pore water and solid particles is the reason behind the generation of thermally-induced  
86 excess pore water pressure of saturated specimen. On other hand, thermally-induced collapse  
87 (*i.e.* rearrangement of soil particles under thermo-mechanical load) of the soil skeleton and  
88 changes in viscosity of the pore water are the impact of temperature on the soils that causes  
89 thermally-induced excess pore water pressure (Campanella and Mitchell, 1968; Schiffmann,  
90 1971). Further, Bai et al., (2021) discussed that the increase in temperature decrease the  
91 effective stress between soil particles and enhance the pore water pressure, which lead to  
92 particle rearrangement of soil. The effect of this particle rearrangement certainly enhance the  
93 growth in volumetric strain. Based on these mechanisms, it can be opined that thermal  
94 consolidation is similar to the primary consolidation of soils (Campanella and Mitchell, 1968;  
95 Shetty et al., 2019). In particular, the creep behaviour of the soil due to the mechanical  
96 loading or unloading prior to the thermal heating can affect the sign (contraction or  
97 expansion) and the magnitude of the change in volume of soils during heating in drained

98 condition (Coccia and McCartney, 2016a). If the secondary compression rate is positive  
 99 (indicating decreasing volume) before heating, thermal volumetric shrinkage is observed for  
 100 normal consolidated soils, whereas if the secondary compression rate is negative (indicating  
 101 increasing volume) prior to heating, thermal volumetric expansion is observed over  
 102 consolidated soil (Burghignoli et al., 2000; Coccia & McCartney, 2016a; Towhata et al.,  
 103 1993). Fig. 1 shows the schematic diagram of secondary compression for NC and OC soil. In  
 104 addition, on the basis of experimental investigations conducted by the earlier researchers, it  
 105 can be stated that the thermal volumetric response of fine-grained soil may be indirectly  
 106 regulated by the over-consolidation ratio (Abuel-Naga, Bergado, & Bouazza, 2007;  
 107 Burghignoli et al., 2000; Campanella & Mitchell, 1968; Hoseinimighani & Szendefy, 2022;  
 108 Vega & McCartney, 2014; Zhu & Qi, 2018).



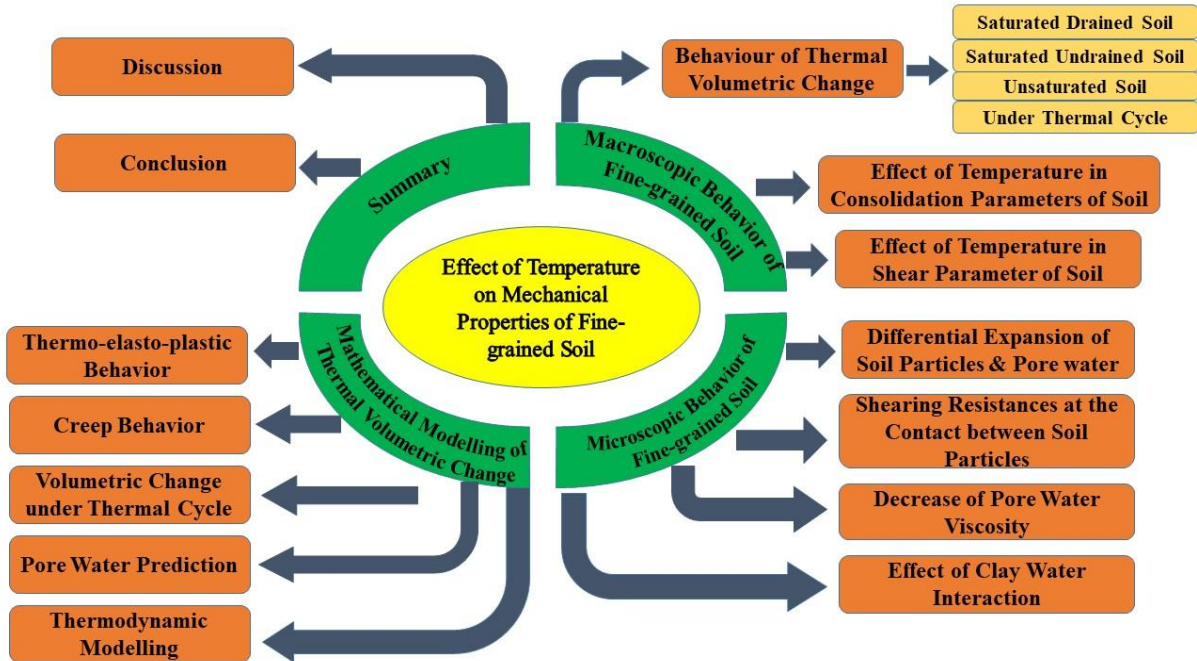
109  
 110 **Fig. 1.** Schematic diagram for secondary compression for NC and OC soil.

111 The application of thermal energy in soil can influence its properties and behaviour.  
 112 Numerous researchers have recognized the effect of thermal energy on properties of fine-  
 113 grained soil such as shear strength, permeability, pore water pressure, consolidation, creep  
 114 index, mineralogical composition, *etc.* This effect is mainly attributed to volumetric change  
 115 of soil against thermo-mechanical loading. In this context, there are a number of recent  
 116 review articles available which have discussed the contemplating issues (Casarella et al.,

117 2021; Hoseinimighani & Szendefy, 2022; Loria & Coulibaly, 2021; Wang et al., 2020) on  
118 this topic. For example, Loria & Coulibaly, (2021) have discussed the thermally-induced  
119 volumetric change of geomaterials and its deriving mechanism. Moreover, Wang et al.,  
120 (2020) have reported the influence on shear strength parameters of fine grained soil against  
121 the application of thermal energy. Furthermore, Casarella et al., (2021) have studied the  
122 effect of temperature on inter-particle forces of fine grained soil and its impact on  
123 macroscopic behaviour. Hoseinimighani & Szendefy, (2022) have discussed the proposed  
124 mechanism and special attention has been given to microstructural alteration, physio-  
125 chemical interaction and possible change at macro scale. Although there is extensive  
126 knowledge about the effect of temperature on the behaviour of fine-grained soil, there is still  
127 a dearth of review which collectively discusses and relates the microscopic, macroscopic, and  
128 theoretical approaches to address this topic. Therefore, this review paper on effect of  
129 temperature on fine-grained soil focuses on three main following aspects:

- 130 - First, the inter-particle forces are summarized for thermal volumetric change of fine-  
131 grained soil at microscopic level. In which diffused double layer (DDL) theory and  
132 particle orientation (e.g.- face to face, edge to face arrangement) are illustrated for a better  
133 understanding of volumetric change at microscopic level.
- 134 - Second, temperature-induced volumetric change and its deriving mechanism are reviewed  
135 separately for saturated and unsaturated soils at the macroscopic level. Subsequently,  
136 thermal volumetric change due to thermal cycle is reported at the macroscopic level.  
137 Moreover, effect of temperature on geotechnical properties of fine-grained soil is also  
138 discussed briefly.
- 139 - Third, additional approaches for modelling of temperature-induced volumetric change of  
140 fine-grained soil are presented.

141 The scope of this paper is to concentrate on the thermo-mechanical behaviour of fine-grained  
 142 soil, where there is novelty and uncertainty due to recent development in thermal interaction  
 143 with soil. The overview of this paper is presented in pictorial form in Fig. 2.



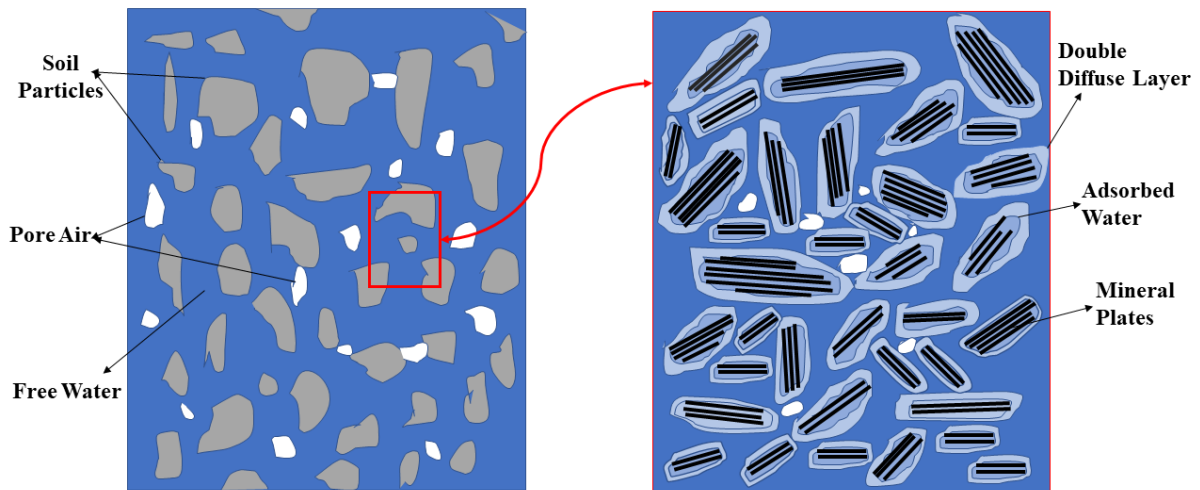
144  
 145 **Fig. 2.** Overview of thermally-induced mechanical behaviour of fine-grained soil.

146 **2. Effect of Temperature on Microscopic Behaviour of Fine-Grained Soil**

147 The microstructural constituents of soil are made up of alumino-silicate oxides in  
 148 presence of water and variable amount of iron and alkali metals. Mineral layers, pore water  
 149 and pore air are deposited in several form in soil. A Schematic diagram of soil structure is  
 150 shown in fig. 3. Water molecules are held by the clay particles through hydrogen bonds due  
 151 to clay's high affinity to water and cations. Therefore, the behaviour of fined grained particles  
 152 is affected by the individual particle and water content in pores. Clay surface has negative  
 153 charge, which adsorbs the positive charge from pore water. By this way, cations are  
 154 distributed over the negatively charged surface, whether density is more near the surface and  
 155 decreased with increase in distance. The cations created a positive charge layer and a double  
 156 layer is formed with negative charge. These layers are termed as diffused double layer, which  
 157 are electrostatically bound to each other. These electrostatic forces control the engineering



158 behaviour of fine grained soil at a large extent. Therefore, thermo-mechanical loading  
159 directly affects the formation of composition and volumetric change of soil by the conversion  
160 and dissipation of energy by phase transformation between liquid phase (i.e.- free water) to  
161 solid phase (i.e.- bound water) (Bai, Zhou, et al., 2021; Bai & Shi, 2017).



162  
163 **Fig. 3.** Schematic diagram of mineralogical structure of soil.

164 The fundamental mechanisms behind the thermally-induced mechanical behaviour of  
165 saturated soils have been perceived in four ways ( Paaswell, 1967; Campanella and Mitchell,  
166 1968; Delage et al., 2000). Each type is described in the following sections.

### 167 **2.1. Thermal expansion of soil particle and pore water**

168 During heating, the discrete components such as soil skeleton and pore fluid of the  
169 soil material expand. The thermal expansion coefficient of water equals to  $207 \times 10^{-6} \text{ }^\circ\text{C}^{-1}$  at  
170  $20 \text{ }^\circ\text{C}$  and increases to  $695 \times 10^{-6} \text{ }^\circ\text{C}^{-1}$  at  $90 \text{ }^\circ\text{C}$  (McKinstry, 1965). Those of some soil  
171 minerals are clay, quartz, calcite and felspar whose thermal coefficient of expansion lie  
172 between  $1$  and  $3 \times 10^{-5} \text{ }^\circ\text{C}^{-1}$  (Mohajerani et al., 2012). Depending on the mineralogy of the soil,  
173 water can expand 7 to 12 times more than solid particle.

### 174 **2.2. Shear resistance at the contact between soil particles**

175           The second mechanism, proposed by (Campanella & Mitchell, 1968; Tarantino et al.,  
176 2021), introduced the effect of temperature on the shear resistance of the contact between soil  
177 particles. The shear resistance of fine-grained soil is separated into two distinct types- micro-  
178 resistance and macro-resistance. Micro-resistance is developed due to inter-particle contacts  
179 of fine-grained soil. The adsorbed water surrounding the soil particles may alter the formation  
180 of inter-particle contacts. During consolidation process, water between soil particles can  
181 dissipate outside due to thermo-mechanical stress. Therefore, heating increases the number of  
182 contacts between particles and thus increases the micro-resistance of fine-grained soil. The  
183 increase in contacts between soil particles are described that the pore water pressure of soil  
184 mass is weaken due to increase in temperature, which causes dissipation of pore water due to  
185 decrease in viscosity of pore water. The formation of micro-resistance is observed for over  
186 consolidated (OC) and normal consolidated (NC) soils with increase in temperature. On the  
187 other hand, macro-resistance is a type of shear strength which is developed due to movement  
188 of soil particles over other in shear plane. Volumetric change has been observed in drained  
189 condition under thermo-mechanical loading, which generates the shear stress due to macro  
190 resistance between particles. Macro-resistance of fine-grained soil would either increase or  
191 decrease with heating. The macro-resistance increases if irreversible volumetric contraction  
192 occurs due to heating, while it decreases if reversible volumetric expansion occurs. On the  
193 other hand, in undrained condition volumetric change is not permitted. Thus, pore water  
194 pressure is developed within soil mass under thermo-mechanical loading in undrained state.  
195 In NC soil, macro-resistance causes positive pore pressure in heating. For OC soil, it causes  
196 negative pore pressure.

### 197 **2.3. Pore water viscosity**

198           It is a well-known fact that viscosity of pore water decreases with increase in  
199 temperature (Paaswell, 1967). The energy of molecules of any substance is defined as the

200 function of temperature as explained by kinetic energy theory. As temperature increases  
201 kinetic energy of soil particles also increases. Therefore, the net attraction force between  
202 molecules decreases, which manifests the decrease in viscosity of soil pore water  
203 (Kuntiwattanakul et al., 1995; Towhata et al., 1993). A lower viscosity of pore water provides  
204 a higher hydraulic conductivity of soil mass. Variation in viscosity for free water under  
205 varying temperature was obtained from experimental results by (Hillel, 2013), which is  
206 written as follows (Eq. 1):

$$207 \quad \mu (T) = -0.00046575 \ln(T) + 0.00239138. \quad (1)$$

208 Where,  $\mu (T)$  is viscosity of water at temperature ' $T(^{\circ}C)$ '.

#### 209 **2.4. Electrostatic force between soil and pore water**

210 Towhata et al., (1993) revealed that a negative charge on the surface of soil solids  
211 would create an electric field with a positive dipole charge of pore water molecule. This  
212 electric field binds neighbouring water molecules to soil grain due to strong electrostatic  
213 forces of attraction, and therefore restricts the motion of pore water molecules. It was further  
214 described that some kinetic energy is associated with each pore water molecule, which is  
215 electrostatically bound to the soil grain surface. When heating is applied, these bound water  
216 molecules may reach the energy threshold and are therefore dissipated from the soil mass.  
217 Temperature therefore appears to affect the clay-water interaction. This clay water interaction  
218 results water to be present in clay in three different forms (Hueckel, 1992; Stępkowska,  
219 1990): (1) Free or bulk water, which flows under hydraulic gradient; (2) Adsorbed water  
220 which forms due to enveloping action between molecules of soil (Hueckel, 1992; Iwata et al.,  
221 2020; Kemper et al., 1964), it cannot flow under gravitational effect; and (3) Hydroxyl or  
222 structural water, which is mainly a part of structural lattice (shape of mineralogical  
223 arrangement) of minerals and cannot leave the lattice below 350 °C. Clay water interaction  
224 can be classified in six different types of molecular interactions viz. water-water, water-

225 cation, water-clay, cation-cation, cation-clay and clay-clay (Casarella et al., 2021; Hueckel,  
226 1992; Iwata et al., 2020; Skipper et al., 1991). Apart from these interaction, physiochemical  
227 internal forces is also developed at the soil particle contacts due to external thermo-  
228 mechanical loading (attraction and repulsion). Hydrate layer at particle surface has been  
229 developed due to equilibrium in physiochemical interaction. Change in thermo-mechanical  
230 loading, disturb the equilibrium balance, which change the thickness of hydrate layer. This  
231 change generates the additional pressure to keep the specimen in equilibrium, which is called  
232 as disjoining pressure. This disjoining pressure is mainly depend upon the rearrangement of  
233 soil particle resulting from physiochemical force and hydrate layer (Golchin et al., 2022a).  
234 Therefore, these potential interactions result in generation of attractive London forces or  
235 dispersion forces, short-range repulsion, and Coulomb force between charged particles,  
236 which can affect the volumetric change in soil lattice (Casarella et al., 2021). Change in  
237 temperature influences the intensity of inter-particle forces in soil lattice, inducing  
238 rearrangement of soil particles. As a result, particle surface and edge accumulate positive and  
239 negative charge correspondingly. Consequently, two different orientations (face-to-face and  
240 edge-to-face) are developed between soil lattices (Casarella et al., 2021; Yong, 1999). In  
241 face-to-face arrangement, negatively charged layer overlaps to adjacent parallel particle in  
242 such a way that a repulsive force generates in between. As a result, inter-particle distance gets  
243 adjusted by both external compressive force and internal repulsive force. Repulsive forces are  
244 directly proportional to temperature and inversely with distance between particles  
245 (Hoseinimighani & Szendefy, 2022). This is mainly due to development of the DLVO  
246 (Derjaguin, Landau, Verveij, and Overbeek) theory. The DLVO stated that the adsorption of  
247 mineral on suspended particle reduced the repulsive force between soil particles and  
248 suspended particle due to decrease in zeta potential (Bai, Nie, et al., 2021). Moreover, due to  
249 increase in temperature the inter-particle distance between particles of face-to-face

250 arrangement also increases for applied external compressive load which causes an expansion  
251 of clay. This expansion would be reversible in nature due to the reverse alteration of  
252 dielectric permittivity to its initial value upon cooling or removal of thermal load (Casarella  
253 et al., 2021; Ghahremannejad, 2003; Pedrotti & Tarantino, 2018). On the other hand, in case  
254 of edge-to-face arrangement, a contact configuration is developed by the Van der Waal's  
255 force of attraction between oppositely charged particles at edge and face respectively.  
256 However, due to increase in temperature, the net attractive force gets weakened. Additionally,  
257 the edge-to-face interaction between particles develop non reversible deformation if the  
258 contact is broken (Casarella et al., 2021).

259         The effect of temperature on diffuse double layer (DDL) remains inconclusive. DDL  
260 insures that soil particles have positive or negative charge on surface due to availability of  
261 charged group within, or attraction of charged layers from surrounding medium. Therefore,  
262 an electrical double layer is established between solid particles and pore water to confirm  
263 electro-neutrality within soil mass. Mitchell & Soga (2005) analysed the Gouy-Chapman  
264 equation and stated that DDL is unaffected by temperature variation. On the contrary, Morin  
265 & Silva, (1984) gathered the experimental results on high-porosity clay and found that the  
266 increase in temperature prone to compress the DDL and decrease the ionic concentration,  
267 which tends to breakdown of adsorbed water. Furthermore, below certain separation of  
268 mineral layers (less than 50 Å) and at low porosity, DDL theory fails to describe the  
269 behaviour of interaction forces (Baldi et al., 1988; Hueckel, 1992). This is mainly caused due  
270 to domination of solvation forces near the surface. This is due to the structural arrangement of  
271 pore water, which creates the potentials of short-range intermolecular pairs different from the  
272 potentials derived from any continuum theory. Solvation force is governed by the geometric  
273 constrain of structural packing imposed by solid particle surface, which is mainly caused due  
274 to the geometric constraints induced by the very thin separation between mineral layers. In

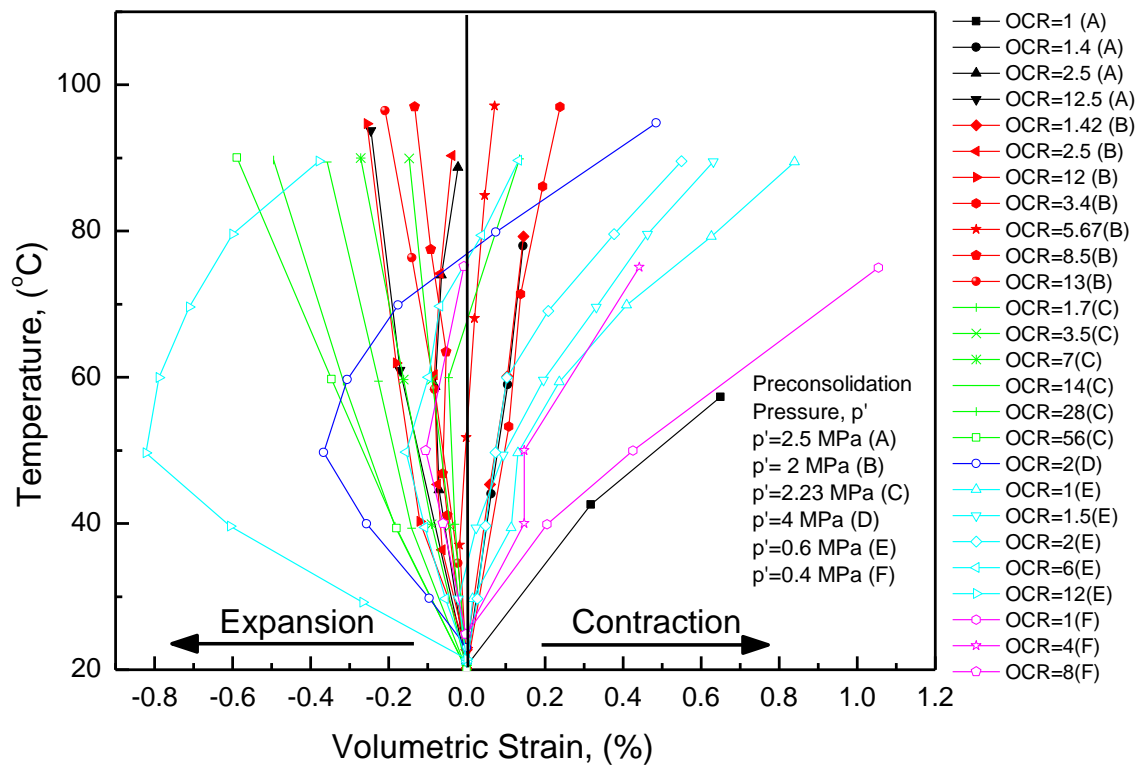
275 such system, repulsive hydration forces gets generated and the bond stress is usually higher  
276 than that estimated by DDL theory (Baldi et al., 1988; Hueckel, 1992; Ma & Hueckel, 1993).

### 277 **3. Effect of Temperature on Macroscopic Behaviour of Fine-Grained Soil**

#### 278 **3.1. Thermally-induced volume change behaviour of saturated soil under drained** 279 **conditions**

280 There are substantial number of studies available which elucidate the volumetric  
281 change of saturated soils due to temperature change under drained conditions (Abuel-Naga et  
282 al., 2007c; Baldi et al., 1988; Delage et al., 2000; Hueckel & Baldi, 1990; Sultan et al., 2002;  
283 Towhata et al., 1993). Baldi et al., (1988) noticed the effect of stress history on the expansion  
284 and contraction of soil specimen when heated beyond the room temperature. Fig. 4 presents  
285 volumetric strain versus temperature during heating from room temperature (close to 20 °C)  
286 at different magnitudes of over consolidation ratio (OCR) value. Data collected on various  
287 soils such as Potinda clay, Pasquasia clay, MC clay, Boom clay and Kaolin clay from  
288 different studies are presented in the same plot for comparison. The results in Fig. 4 reveal  
289 that Kaolin clay for high magnitude of OCR (i.e., 6, 12) expands up to a certain temperature,  
290 beyond which it contracts. Similar pattern can be identified for MC clay. Hence, this unique  
291 temperature is termed as transition temperature (Baldi et al., 1988). The transition  
292 temperature increased with increase in over consolidation ratio (Hoseinimighani & Szendefy,  
293 2022). Moreover, thermal contraction is detected for lightly over consolidated sample from  
294 the beginning of heating such as Pontida clay for OCR = 1 and 1.4, Pasquasia clay for OCR =  
295 1.4 and 2.5, and Boom clay for OCR = 2. However, only few soil specimens such as Pontida  
296 clay at OCR = 2.5, Pasquasia clay at OCR = 3.4 and MC clay at OCR = 3.4 show expansion  
297 on initial heating and contraction on further heating. Few discrepancies have also been  
298 observed in literature. Laloui & Cekerevac, (2003) have reported that transition temperature  
299 is not affected by over consolidated ratio, all OCR specimens are transiting almost at constant

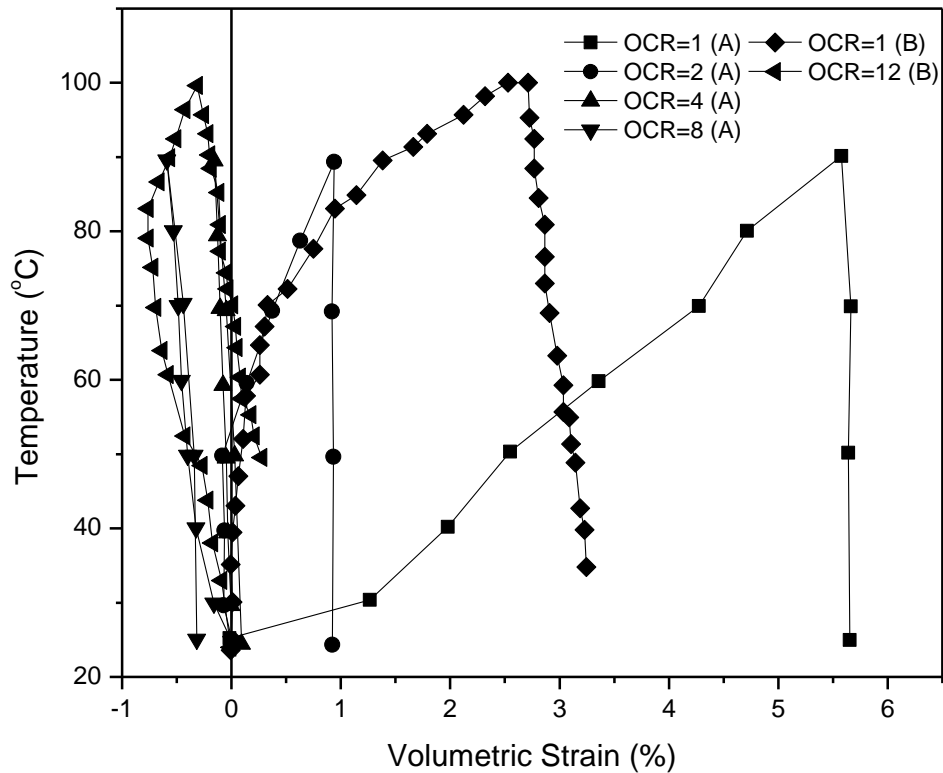
300 temperature from expansion to contraction. Bai et al., (2019) have also reported the effect of  
 301 OCR due to heating. It was reported that the soil showed contraction for OCR 1 and 4 and  
 302 expansion for OCR 8. It has been reported from fig 4 that plastic volumetric strain is  
 303 observed for OCR value less than 2. Moreover, elastic volumetric strain has been observed  
 304 for OCR value greater than 2. As the OCR value increases the elastic volumetric strain also  
 305 increases due to heating.



306  
 307 **Fig. 4.** Volumetric behaviour of saturated soils during heating: (A) Potinda clay (Baldi et al.,  
 308 1988), (B) Potinda and Pasquasia clay (T. Hueckel & Baldi, 1990), (C) MC Clay (Towhata et  
 309 al., 1993), (D) Boom Clay (Delage et al., 2000), (E) Kaolin clay (Cekerevac & Laloui, 2004)  
 310 and (F) Saturated Clay (Bai et al., 2019b).

311 Subsequently, few studies have also performed heating under drained conditions with a  
 312 heating/cooling path (Abuel-Naga, Bergado, Bouazza, et al., 2007; Sultan et al., 2002). Fig. 5  
 313 depicts the thermal volumetric change against a thermal cycle in drained state. It is opined  
 314 that the thermal irreversible volumetric change of normally-consolidated specimens is  
 315 independent of applied stress. Thermal volumetric change for over-consolidated soil is  
 316 observed as reversible in nature. Higher the OCR value, large portion of reversible

317 volumetric strain is observed. Moreover, several researchers identified that soil specimen  
 318 undergoes from expansion during heating to contraction during the subsequent cooling  
 319 (Towhata et al., 1993; Sultan et al., 2002, Abuel-Naga et al., 2008; Coccia and McCartney,  
 320 2012).



321  
 322 **Fig. 5.** Thermal volumetric change of saturated soil during thermal cycle; (A) Bangkok clay  
 323 (Abuel-Naga, Bergado, Bouazza, et al., 2007), (B) Boom clay (Sultan et al., 2002).

324 The macroscopic thermally-induced volumetric change of fine-grained soil can be  
 325 interpreted using knowledge on microscopic behaviour. In saturated soil mass, water particles  
 326 and soil particles are bound by electrostatic force, which restrict the motion of pore water  
 327 from soil. During heating, every particle gains some kinetic energy, which weaken this  
 328 electrostatic bond between soil particles and pore water. With this in view, the viscosity of  
 329 pore water is reduced and dissipation of water takes place due to thermo-mechanical loading.  
 330 A major observation from the results is that a NC soil undergoes almost irreversible  
 331 contraction during a heating/cooling, and reversible expansion has been observed for highly  
 332 OC soil. Actually, under NC condition, a compressive rearrangement of soil particles take

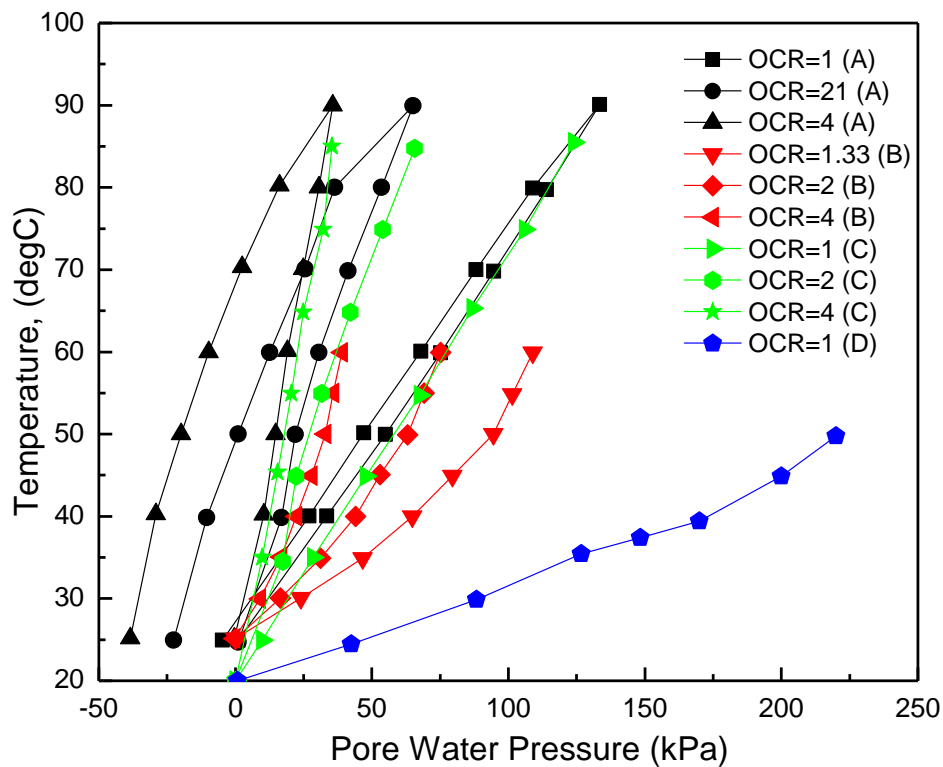


333 place until a shear bond between soils particles are developed to withstand with stress at  
334 higher temperature. As at NC, the shear stress at the particles contacts is already close to the  
335 shear resistance, heating decreases the shear resistance at the particles contacts and induce  
336 irreversible collapses. Under OC condition, thermal heating cannot produce rearrangement of  
337 soil particles because it is more stable and exposed to lower mobilized force. Therefore, OC  
338 soil undergo into reversible thermo-elastic expansion up to certain temperature. However,  
339 heating beyond a certain temperature for OC soil weakens the shear resistance between soil  
340 particles, which lead to irreversible contraction of soil specimen.

### 341 **3.2. Thermo-mechanical behaviour of saturated soils under undrained conditions**

342 Numerous studies have been carried out against thermo-mechanical behaviour of fine-  
343 grained soil under undrained conditions (Abuel-Naga, Bergado, & Bouazza, 2007; Ghaaowd  
344 et al., 2015; T. Hueckel & Pellegrini, 1992; Mohajerani et al., 2012; Uchaipichat & Khalili,  
345 2009). Thermally-induced pore water pressure increases with increase in temperature and this  
346 increase is less significant at a higher OCR value (Abuel-Naga, Bergado, & Bouazza, 2007;  
347 T. Hueckel & Pellegrini, 1992). (Abuel-Naga, Bergado, & Bouazza, 2007; Ghaaowd et al.,  
348 2015; Mohajerani et al., 2012; Uchaipichat & Khalili, 2009) have performed heating tests  
349 under undrained conditions on consolidated specimens at different OCR values. Fig. 6  
350 illustrates the thermally-induced excess pore water pressure as a function of temperature.  
351 Abuel-Naga et al., (2007) have carried out undrained heating/cooling test on Bangkok clay  
352 and observed that thermally-induced pore water pressure for NC soil shows reversible trend,  
353 while OC soil shows irreversible trend with negative pore water pressure. Furthermore,  
354 Uchaipichat & Khalili, (2009) have conducted the undrained heating of saturated specimen  
355 with different effective stress on silty soil. Pore-water pressure of soil increases with increase  
356 in temperature as well as effective stresses. Moreover, Ghaaowd et al., (2015) have analyzed  
357 the pore water pressure for kaoline clay for OCR value equal to 1 and observed that pore

358 water pressure increases with increase in temperature. Subsequently, effective stress and  
 359 shear resistance of adsorbed water decrease related to heating. Therefore, reversible  
 360 thermally-induced pore water pressure can be observed for NC soil (Abuel-Naga, Bergado, &  
 361 Bouazza, 2007). On the other hand, for OC soil Pusch et al., (1991) illustrated that thermally-  
 362 induced pore water pressure in specimen would cause unstable stress within soil mass due to  
 363 increase in kinetic energy of particles, which resulting rearrangement of soil particles to  
 364 improve uniformity. Therefore, it can be opined that for OC soil thermally-induced pore  
 365 water pressure becomes irreversible in nature due to rearrangement of particles within soil  
 366 mass.



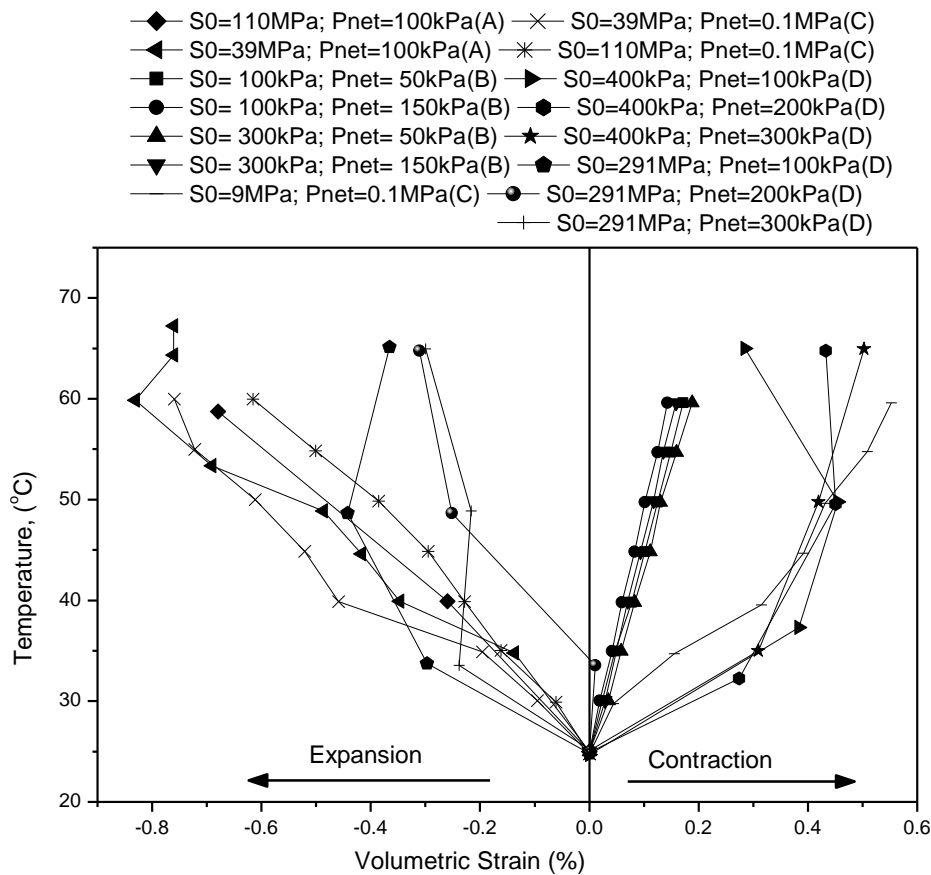
367 **Fig. 6.** Thermal effect on pore water pressure of soil; (A) Bangkok Clay (Abuel-Naga,  
 368 Bergado, & Bouazza, 2007), (B) Silt (Uchaipichat & Khalili, 2009), (C) Bangkok Clay  
 369 (Ghaaowd et al., 2015), (D) Kaoline Clay (Ghaaowd et al., 2015).

### 371 3.3. Volume change behaviour of unsaturated soil

372 Several researchers investigated the volumetric behaviour of unsaturated fine-grained  
 373 soil under thermo-mechanical loadings (Romero et al., 2005; Salager et al., 2008; Tang et al.,  
 374 2008; Uchaipichat and Khalili, 2009; Alsherif and McCartney, 2015; Coccia and McCartney,

2016a, 2016b;). It can be perceived from the literature that unsaturated soil results are also similar to that of saturated soil (Salager et al., 2008; Uchaipichat and Khalili, 2009). Fig. 7 illustrates the result of volumetric strain during heating of unsaturated samples at different suctions and net stresses. Fig. 7 states that the thermal dilation of the sample increases with increase in matric suction and decreases with increase in net stresses (Uchaipichat and Khalili, 2009). Tang et al., (2008) performed a thermo-mechanical experimental investigation on compacted bentonite specimen with different suctions, in a temperature-controlled isotropic cell. Subsequently, it was shown that the expansion of the soils was induced due to heating at low stress (i.e., high OCR) and high suction. Conversely, contraction was reported while heating at high stress (i.e., low OCR) and low suction (Tang et al., 2008). Moreover, Uchaipichat and Khalili, (2009) conducted thermo-mechanical tests on different silt samples of varying initial suction (i.e., 100 and 300 kPa) at different confining pressures (i.e., 50 and 150 kPa). It can be observed that upon heating, the specimen with lower confining stress experienced expansion and for higher confining stress, contraction was observed (Uchaipichat and Khalili, 2009). This study stated that pre-consolidation stress of sample increases with increase in suction magnitude. Hence, as suction value increases, the OCR value also increases. Therefore, thermal collapse is insignificant for over consolidated sample and increases with decrease in over consolidation ratio (Uchaipichat and Khalili, 2009). Furthermore, Salager et al., (2008) conducted an experimental study to explore the mechanical behaviour at different temperature and suction values of Sion Silt. The results demonstrated that temperature has not a significant effect on the compressibility of soil. On the other hand, compressibility of soil is decreased with increase in suction level. However, the apparent pre-consolidation stress is affected by the applied temperature and suction. Similarly, Coccia and McCartney, (2016a) have performed the thermo-mechanical tests at three different stages: i.e. 1) Matric suction level; 2) Isotropic compression under constant

400 rate of strain; and 3) drained heating. Through this study, efforts have been made by (Alsherif  
 401 & McCartney, 2015; Coccia & McCartney, 2016a) to investigate the influence of secondary  
 402 consolidation on thermal volume change response of bonny silt and the role of stress history  
 403 and loading pattern on thermal volumetric response of the soils. Decrease in viscosity of pore  
 404 water in soil mass reduces the interfacial tension between pore water and soil particles due to  
 405 heating (Romero et al., 2005). This reduction in interfacial tension may also accelerate the  
 406 rate of secondary creep due to the reduction in the applied load to the soil transfers to the  
 407 grain-to-grain contacts (Coccia & McCartney, 2016a, 2016b).



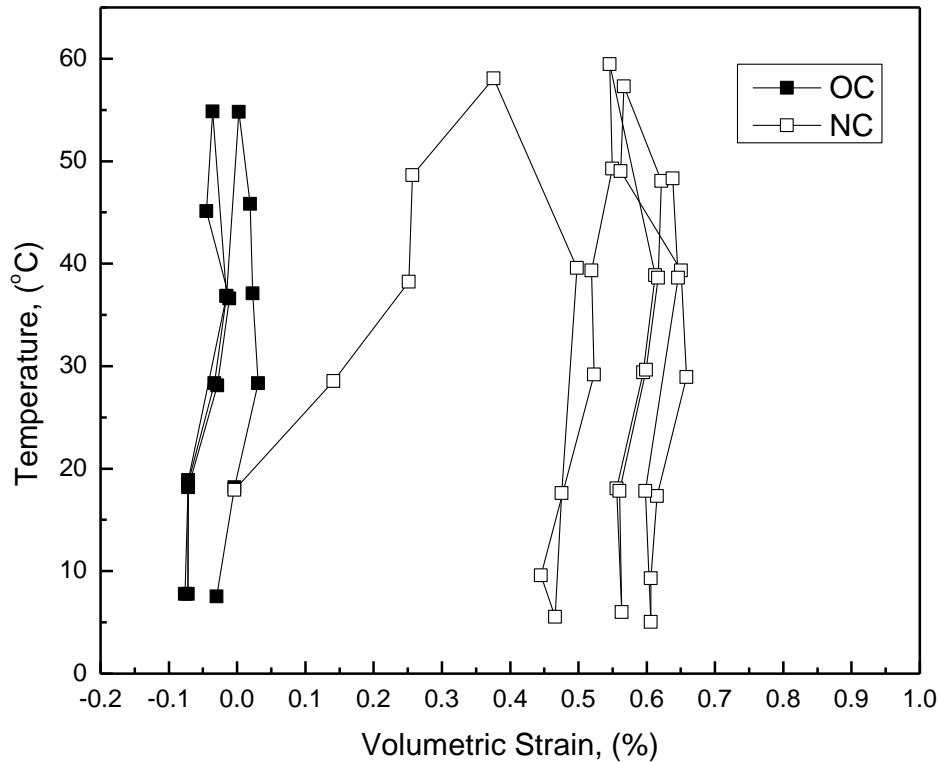
408  
 409 **Fig. 7.** Volumetric behaviour of unsaturated soils during heating: (A) Bentonite (Tang et al.,  
 410 2008), (B) Silt (Uchaipichat & Khalili, 2009), (C) Bentonite (Y.-J. Cui et al., 2011) and (D)  
 411 Silt (Alsherif & McCartney, 2015).

412 **3.4. Volumetric change under thermal cycles**

413 A cyclic thermal loading on a saturated fine-grained soils for NC and OC soil

414 condition causes thermo-elasto-plastic response and thermo-elastic response, respectively  
415 during heating (Di Donna and Laloui, 2015). Several researchers stated that for  
416 approximately 10 cycles of heating and cooling, an additional irreversible contraction is  
417 generated for NC and slightly OC soil before approaching to reversible behaviour which is  
418 expansive for heating and compressive for cooling (Bai & Shi, 2017; Di Donna & Laloui,  
419 2015; Loria & Coulibaly, 2021; Mu et al., 2019; Zhang, 2017). Initially, expansion was  
420 observed due to the expansion of solid grains and pore water, then the pore water started  
421 draining with dissipation of pore pressure which led to change in volumetric strain (Bai &  
422 Shi, 2017). Although, accumulation behaviour of volumetric strain was developed on  
423 sequential temperature cycles (refer fig. 8). The magnitude of compression, which was  
424 developed on soil under thermal cycles, increased with increase in clay content (Loria &  
425 Coulibaly, 2021; Mu et al., 2019). As a result, the friction force at the inter-particle contacts  
426 decreases with increasing temperature., the friction force at the inter-particle contacts  
427 decreases with increasing temperature, which causes partial collapse of the soil structure.  
428 After this collapse, inter-particle equilibrium is again reached, when the number of additional  
429 contacts created between the particles is sufficient to transfer the imposed thermal stress.  
430 Bond slippage is more likely when the contact position is close to a failure condition, which  
431 is the case for NC materials. This is mainly driven by the particle rearrangement, which  
432 associated due to expansion of soil grains against thermo-mechanical loading (Di Donna &  
433 Laloui, 2015). Therefore, gradual collapse of soil structure which leads to continuous drop in  
434 void ratio until further stress bond develops between soil particles at higher temperature. This  
435 phenomenon is totally irreversible, hence expressed as thermal secondary compression. After  
436 successive temperature cycles, there is no sign of volume change under secondary  
437 compression because the specimen has already been recomposed with earlier temperature  
438 cycles (Campanella and Mitchell, 1968). Under OC conditions, the rearrangement of particles

439 is more limited, and the thermo-elastic expansion of the components predominates. When  
 440 considering the cyclic thermal load on the NC soil, the configuration becomes more stable  
 441 with each cycle depending on the amount of accumulated plastic strain, and the available  
 442 space for additional failure decreases.

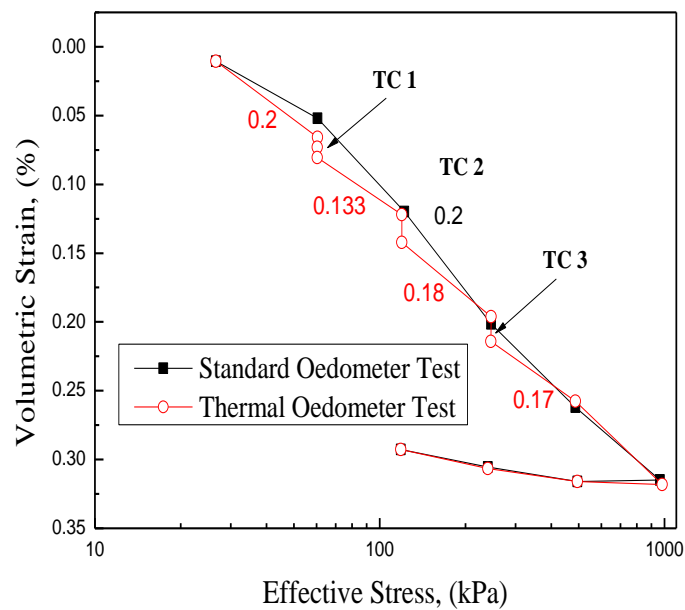


443  
 444 **Fig. 8.** Volumetric change of soil under thermal cycles (Q. J. Ma et al., 2017).

445 **3.5. Thermal hardening**

446 Apart from that, the effect of temperature cycles on soil compressibility was analysed  
 447 in various studies. In this regard, Shetty et al., (2019) performed a series of experiments on  
 448 fine grained soil, which was exposed to sequential thermo-mechanical stress. This signifies  
 449 that, the specimen first experienced mechanical stress and subsequently temperature cycle  
 450 was applied. Fig. 9 shows the relation between volumetric strain and effective stress. A  
 451 change in volumetric strain was noticed when specimen was imposed to temperature cycle.  
 452 The cumulative temperature-induced volumetric strain has been defined as the sum of  
 453 volumetric strains for each temperature cycle. Moreover, the change in slope caused by

454 imposition of temperature cycle designates that the compressibility of specimen along the  
 455 sequential thermo-mechanical path decreases on exposure to temperature cycle. This would  
 456 basically escalate the stiffness ( $E$ ) and hardness ( $H$ ) of soil solids due to application of  
 457 temperature cycle (Shetty et al., 2019). Similarly, (Kadali et al., 2013) have also used nano-  
 458 indentation technique to investigate the effect of temperature on stiffness ( $E$ ) and hardness  
 459 ( $H$ ) of several fined grained soils. The change in stiffness and hardness of soil specimen due  
 460 to temperature cycle has been reported by various research studies (Plum and Esrig, 1969;  
 461 Cui et al., 2000; Abuel-Naga et al., 2007c). Furthermore, it has been stated that exposure to a  
 462 temperature cycle, at a particular effective stress, has no impact on the volumetric strain due  
 463 to temperature experienced by the specimen on subsequent thermal cycle at a higher effective  
 464 stress. Similarly, Ma et al., (2017) have perceived that decrease in volumetric strain of the  
 465 specimen is observed when it is exposed to repeated thermal cycles at a specific stress.

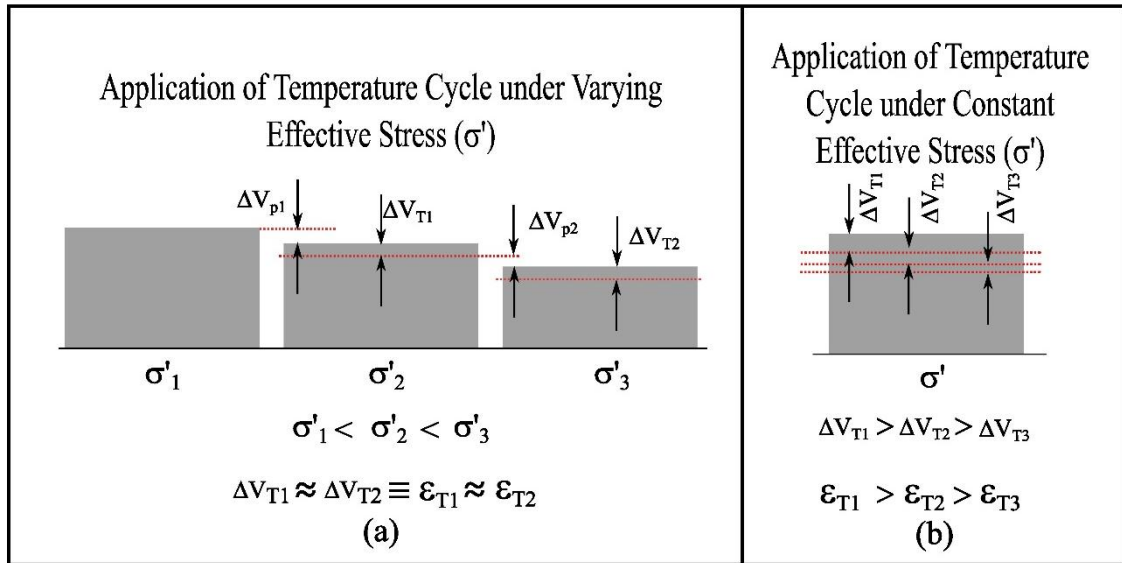


466  
 467 **Fig. 9.** Effect of TCs on Volumetric Strain with Effective Stress (Shetty et al., 2019)

468 Additionally, numerous researchers (Salager et al., 2008; Tang et al., 2008;  
 469 Uchaipichat and Khalili, 2009) examined the effects of suction, effective stress, and OCR on  
 470 the unsaturated soil at different temperatures. Unreported in the literature as of yet is the

471 study on unsaturated fine-grained soil under cyclic temperature. Additionally, it has been  
472 suggested that fluctuation in pore water pressure is seen at various effective stresses when the  
473 saturated specimen is exposed to a temperature cycle (Bai & Shi, 2017). Due to the expansion  
474 of the pore water and solid grains during rapid heating, the pore water pressure increases until  
475 it reaches its maximum value. Again pore water drainage causes pore water pressure to  
476 decrease to zero. Due to water absorption, pore water pressure decreases to a negative value  
477 during cooling before returning to zero (Bai & Shi, 2017). Due to the increase in effective  
478 stress, the amplitude of pore pressure therefore decreases over successive heat cycles.  
479 Additionally, it is said that the saturated specimen experience identical volumetric strain  
480 under variable effective stress during consecutive temperature cycles (Shetty et al., 2019).  
481 The similar trend has been depicted in Fig. 10(a) (application of TC under varying  $\sigma'$ ) and  
482 Fig. 10(b) (application of TC under constant  $\sigma'$ ). However, in Fig. 10(a), the soil matrix is  
483 loaded to varying effective stress, which increases after imposition of each TC. This results in  
484 same degree of the structural rearrangement of the sample due to thermal cycle under the  
485 varying  $\sigma'$ . Therefore, the volumetric change remains constant under each TC (i.e.-  
486  $\Delta V_{T1}, \Delta V_{T2}$  and  $\Delta V_{T3}$ ), and thus the volumetric strain achieved in the subsequent TC remains  
487 unchanged (i.e.-  $\Delta \varepsilon_{T1} \approx \Delta \varepsilon_{T2}$ ) (Q. J. Ma et al., 2017; Shetty et al., 2019). There are several  
488 studies that applied a repetitive TC on specimen on constant  $\sigma'$ , which reduce the extent of  
489 structural rearrangement in each successive TC, hence the magnitude of volumetric change  
490 decreases with each consecutive TC (i.e.-  $\Delta V_{T1} > \Delta V_{T2} > \Delta V_{T3}$ ) (Campanella and Mitchell,  
491 1968; Ma et al., 2017). It would result in lower generation of pore pressure due to thermal  
492 stress and the same is responsible to decrease in volumetric strain (refer Fig. 10(b)).





493

494 **Fig. 10.** Effect of temperature cycle on soil compressibility (a) under varying effective stress  
495 and (b) under constant effective stress.

496 **3.6. Thermal dependent creep behaviour**

497 Soft clays manifest time-dependent behaviour due to their viscosity. Prolonged  
498 deformation of these clays after dispersing excess water pressure from the pores, is called as  
499 creep deformation. Creep behaviour of clay is vigorously associated with bond elimination  
500 due to application of mechanical stress (Yin et al., 2017; Zhu et al., 2017) and change in  
501 temperature (Houston et al., 1985; Fox and Edil, 1996; Laloui et al., 2008; Coccia and  
502 McCartney, 2016a; Li et al., 2018; Zhu and Qi, 2018; Jarad et al., 2019). Houston et al.  
503 (1985) have shown that the rate of volumetric creep increases at elevated temperature.  
504 increase in volumetric creep rate with upraising the temperature has also been established.  
505 Likewise, Fox and Edil (1996) have also described the increment of creep coefficient under  
506 induced temperature. Based on the experimental results, thermal creep coefficient varies  
507 linearly with the temperature (Plum and Esrig, 1969). Furthermore, Jarad et al., (2019) have  
508 performed experiments to determine the creep coefficient for two specimen of clay soils. The  
509 results have indicated that the creep index increased with heating. Besides, it has been  
510 mentioned that the clay of lower dry density has a higher creep index. At a higher

511 temperature, the decrease in the apparent viscosity of the contacts between the particles and  
512 pore water would increase creep. Other reasons can be due to the weak particle bonding or  
513 inter particle shear strength at high temperatures, and therefore the strain increases with  
514 increasing temperature (Jarad et al., 2019). Subsequently, the variation in creep rate of soil  
515 due to heating is evaluated due to change in bond between particles or due to irreversible  
516 internal deformation in orientation of soil (Li et al., 2018).

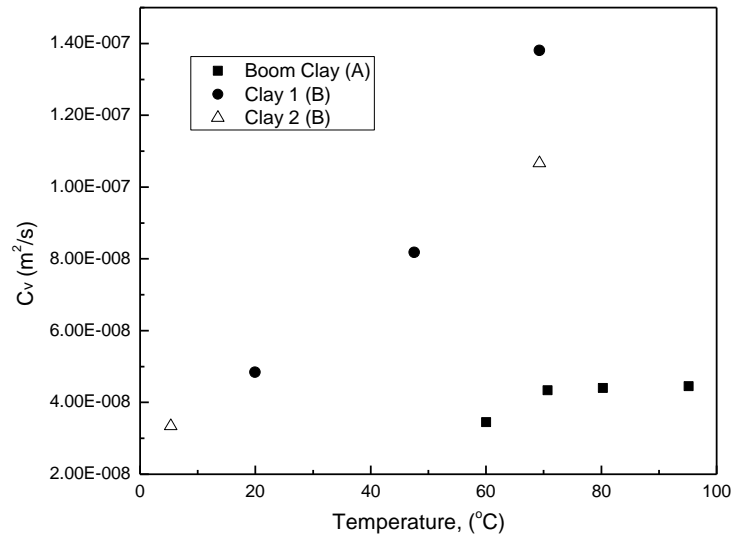
### 517 **3.7. Coefficient of consolidation**

518 In some studies, the consequences of temperature change on the coefficient of  
519 consolidation ( $C_v$ ) were illustrated and it was stated that this coefficient depends on  
520 temperature and vertical effective stress (Delage et al., 2000; Favero et al., 2016; Jarad et al.,  
521 2019; Ogawa et al., 2020). After synthesis of the obtained results, the coefficient of  
522 consolidation is higher at a higher temperature (Fig. 11). Moreover, Terzaghi, (1923)  
523 developed a relation among the volume compressibility ( $m_v$ ), permeability ( $k_s$ ) and the  
524 coefficient of consolidation ( $C_v$ ) in the theory of one dimensional consolidation, which is  
525 extracted in Eq. 2:

$$526 \quad C_v = \frac{k_s}{m_v \gamma_w} \quad (2)$$

527 Where,  $\gamma_w$  is unit weight of water. It has been mentioned earlier that the permeability  
528 increases with increase in temperature. This phenomenon occurs due to the decrease in the  
529 viscosity of the pore water with increase in temperature, which can be calculated from eq. 1.  
530 Thereby, it leads to increasing the dissipation of the excess pore water pressure and,  
531 therefore, the consolidation process also expedites (Towhata et al., 1993; Di Donna and  
532 Laloui, 2015). Hence, coefficient of consolidation is also higher for a higher temperature. In  
533 addition, the influence on the coefficient of volume compressibility ( $m_v$ ), which basically  
534 reflects the compressibility of specimen, was evaluated for different temperature and  
535 consolidation pressure (Bag and Rabbani, 2017; Jarad et al., 2019). It has been further

536 explored that at a constant consolidation pressure, the volume compressibility shows  
 537 insignificant change with respect to temperature. Since, the volume compressibility decreases  
 538 with increase in consolidation pressure, it can be opined that the volume compressibility  
 539 strongly depends upon imposed consolidation pressure (Bag and Rabbani, 2017).



540  
 541 **Fig. 11.** Variation of Coefficient of Consolidation with Temperature (A) Delage et al., (2000)  
 542 and (B) Jarad et al., (2019).

543 Alteration in permeability of fine grained soil as an influence of temperature has been  
 544 illustrated by several researchers (Cho et al., 1999; Ye et al., 2012; Mon et al., 2014; Jarad et  
 545 al., 2019). Abuel-Naga et al., 2006 have conducted the permeability test on soft Bangkok clay  
 546 under elevated temperature. The result indicated that the increase in soil temperature also  
 547 increased the permeability of soil. This could be due to alteration in viscosity and unit weight  
 548 of pore water. Permeability of soil can be evaluated by the eq. 3, which is a relation between  
 549 viscosity and unit weight of water, and it can also be measured from direct permeability test  
 550 at different temperature.

$$551 \quad \frac{K(T)}{K(T_o)} = \frac{\mu(T_o)\gamma_w(T)}{\mu(T)\gamma_w(T_o)} \quad (3)$$

552  $K(T)$  and  $K(T_o)$  is defined as the permeability at temperature,  $T$  and room temperature  $T_o$ ,  
 553 respectively.  $\mu(T)$  and  $\mu(T_o)$  is defined as viscosity of pore water at temperature  $T$  and room  
 554 temperature  $T_o$ , respectively, which can be calculated from eq. 1.  $\gamma_w(T)$  and  $\gamma_w(T_o)$  is

555 defined as unit weight of pore water at temperature  $T$ , and room temperature  $T_o$ , respectively.  
556 Likewise, Delage et al., (2000) have also adopted eq. 3 to study the effect of temperature on  
557 permeability. Besides, Jarad et al., (2019) have also conducted tests at different temperature  
558 to explore the variation in intrinsic permeability of soil. Based on these literatures, it can be  
559 established that permeability is proportional to the temperature due to decrease in viscosity of  
560 pore water at elevated temperature. But the intrinsic permeability, which is a function of  
561 porosity, is independent of temperature. It has also been conveyed that the dissipation of pore  
562 water pressure is higher at a higher temperature (Delage et al., 2000; Jarad et al., 2019).

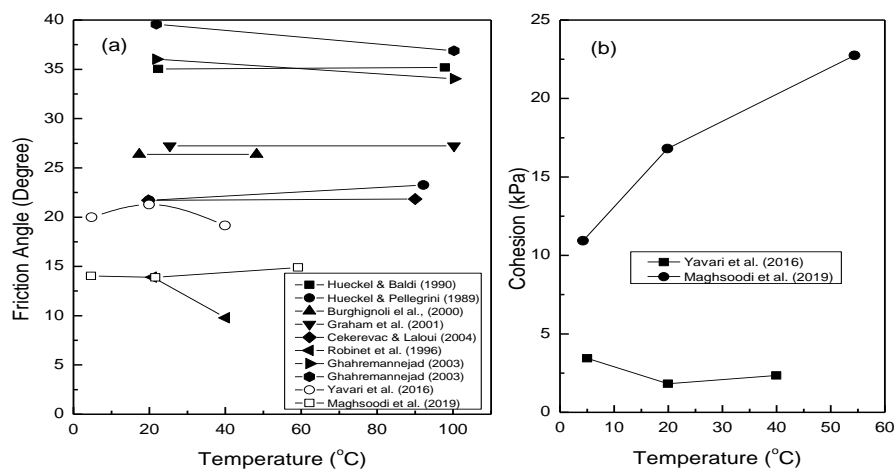
### 563 **3.8. Shear strength parameters**

564 Despite of having several extensive studies, impact of temperature on shear strength  
565 of soil remains a contentious matter, which needs to be discussed clearly due to diverse  
566 response obtained from several studies (Abuel-Naga, Bergado, & Lim, 2007; Campanella &  
567 Mitchell, 1968; Cekerevac & Laloui, 2004; Maghsoodi et al., 2020, 2021; Wang et al., 2020;  
568 Yavari et al., 2016). An increase in shear stress upon heating in drained and undrained  
569 conditions has been found for Bangkok clay irrespective of OCR value (Abuel-Naga et al.,  
570 2007b). (Campanella & Mitchell, 1968; T. Hueckel & Baldi, 1990; Kuntiwattanukul et al.,  
571 1995; Maghsoodi et al., 2020) have also reported an increase in shear strength with increase  
572 in temperature. While, (Burghignoli et al., 2000; Cekerevac & Laloui, 2004; Graham et al.,  
573 2001; Towhata et al., 1993; Yavari et al., 2016) have observed that shear strength remains  
574 unchanged upon heating. On the other hand, several researches reported decrease in shear  
575 strength upon heating (Ghahremannejad, 2003; T. Hueckel & Borsetto, 1990; Lingnau et al.,  
576 1996). For NC soil, a compressive deformation has been reported during heating, which is  
577 irreversible in nature. This is mainly caused by rearrangement of soil particles, which  
578 improve the contact bond between particles thus shear strength should be increased.  
579 Similarly, couple of studies Abuel-Naga et al., (2007b) have reported increase in shear

580 strength of soil with drained heating condition for Bangkok clay and Kaolin clay,  
581 respectively. Moreover, Kuntiwattanakul et al., (1995) have performed undrained shear  
582 strength tests under heating condition and increase in shear strength is reported. Nonetheless,  
583 few researchers claimed decrease in shear strength under undrained heating (Laguros, 1969;  
584 Sherif and Burrous, 1969; Hueckel and Borsetto, 1990; Ghahremannejad, 2003). Baldi et al.,  
585 (1988) explained that this thermo-elasto-plastic stress could lead to microstructural changes  
586 of soils, which create the contact between particles and creates irreversible stress for NC soil.  
587 For OC soil, Kuntiwattanakul et al., (1995) have explained that shear strength of soil  
588 increases with increase in temperature when micro-resistance dominates. Micro resistance  
589 arises due to bonding between inter-particle contact of solid-solid. In micro-resistance,  
590 contact between soil particles increases due to increase in temperature. Moreover, shear  
591 strength of soil decreases with increase in temperature for OC soil when macro-resistance  
592 dominates. Macro resistance arises due to the movement of clay particles over other in shear  
593 plane. Macro-resistance would decrease the shear strength when temperature rise induces a  
594 volumetric expansion.

595 Subsequently, the shear strength parameters with elevated temperature has been  
596 evaluated by several researchers (Hueckel and Baldi, 1990; Robinet et al., 1996; Burghignoli  
597 et al., 2000; Graham et al., 2001; Ghahremannejad, 2003; Yavari et al., 2016; Maghsoodi et  
598 al., 2020). It can be noted that the effect of temperature on friction angle is insignificant, and  
599 no clear trend has been reported. Similarly, cohesion of clayey soil is increased for kaolin  
600 with increase in temperature (Maghsoodi et al., 2020) however reverse result is also reported  
601 by Yavari et al., (2016). The effect of temperature on shear strength parameter is summarized  
602 in Fig. 12. In drained heating condition of soil, contraction of sample occurred, subsequently  
603 shear strength increased due to thermal hardening phenomena. Due to this, thermally induced  
604 irreversible contraction and increase in shear strength observed for NC soil. The reason for

605 this thermo-plastic stress may lie in micro-structural changes because the tendency of soils to  
 606 group together is simulated which increases mineral-to-mineral interaction and generates  
 607 irreversible stress. Therefore, it can be opined that the influence on the shear strength of soil  
 608 with respect to different temperatures is dependent upon the thermal loading history, loading  
 609 path adopted, mineralogical composition and behaviour of soil. Therefore, further  
 610 investigations are requisite to understand clearly the effect of temperature on shear strength  
 611 of the soil.



612 **Fig. 12.** Effect of Temperature on (a) Friction Angle and (b) Cohesion of Soil.  
 613

614 **4. Mathematical Modelling of Thermally-Induced Volumetric Change**

615 This section unveils the studies regarding the modelling approach of thermally-  
 616 induced volumetric change of fine-grained soil. Several researchers have adopted the  
 617 mathematical model to define the thermal volumetric change with respect to different  
 618 behaviour such as – thermo-elasto-plastic behaviour, creep behaviour and thermal  
 619 stabilisation under temperature cycle. Therefore, these modelling aspects are briefly  
 620 discussed in the following sections.

621 **4.1. Elastic strains**

622 Thermo-elasto-plastic volumetric change can take place due to change in temperature  
 623 and mean effective stress. The first thermo-elastic model was described for saturated soil by

624 thermal softening mechanism (Hueckel and Borsetto, 1990). There are several consecutive  
 625 models available for thermo-elastic behaviour of fine grained soil (Abuel-Naga et al., 2007c;  
 626 Cui et al., 2000; Hong et al., 2013; Laloui & François, 2009; Yao & Zhou, 2013; Zhu et al.,  
 627 2021). Several researchers (Y. J. Cui et al., 2000; Hong et al., 2013, 2016; Laloui &  
 628 François, 2009; Zhu et al., 2021) have proposed a model for elastic volumetric strain, which  
 629 is mentioned in eq. 4.

$$630 \quad d\varepsilon_v^e = \alpha dT + \frac{dp'}{K} \quad (4)$$

631 Similarly, (Abuel-Naga, Bergado, Bouazza, et al., 2007) have also proposed a model  
 632 regarding elastic volumetric strain considering the effect of temperature and stress, both,  
 633 which is written in eq. 5.

$$634 \quad d\varepsilon_v^e = \frac{\alpha'}{T} dT + \frac{dp'}{K} \quad (5)$$

635 Where,  $\alpha$  and  $\alpha'$  is termed as volumetric thermal expansion coefficient of soil for eq. 4 and  
 636 eq. 5, respectively.  $T$  and  $p'$  are temperature and effective stress, respectively.  $K$  is defined as  
 637 bulk modulus which is independent of temperature. It is noteworthy to notice that (Abuel-  
 638 Naga, Bergado, Bouazza, et al., 2007) have developed logarithmic equation versus  
 639 temperature for elastic volumetric strain (refer Eq. 5). On this note,  $\alpha'$  is a dimensionless  
 640 quantity, on contrary  $\alpha'$  should have dimension inverse of temperature. Although,  $\alpha$  could be  
 641 a function of temperature and stress (Yao & Zhou, 2013). However, it is essentially  
 642 considered as constant for simplicity (Cui et al., 2000; Hong et al., 2013; Hong et al., 2016;  
 643 Yao & Zhou, 2013; Zhu et al., 2021). Still, (Abuel-Naga, Bergado, Bouazza, et al., 2007)  
 644 have developed an equation for  $\alpha'$ , which varies logarithmically with mean effective stress as  
 645 follow (Eq. 6).

$$646 \quad \frac{d\alpha'}{\alpha'} = b \frac{dp'}{p'} \quad (6)$$

647 Where,  $b$  is soil parameter as a function of microscopic and mineralogical configuration of  
 648 clay. Moreover, (Laloui & François, 2009) have also developed an equation of  $\alpha$ , which  
 649 varies with temperature and OCR, both (refer Eq. 7)

$$650 \quad \alpha = [\alpha_o + \zeta(T - T_o)] \frac{p'_{c0}}{p'} \quad (7)$$

651 Where,  $\alpha_o$  is coefficient of thermal expansion at  $T_o$ ;  $\zeta$  is defined as slope of variation  $\alpha$  with  
 652  $T$ .  $p'_{c0}$  is pre-consolidation pressure at  $T_o$ . The bulk modulus is considered same as Cam-clay  
 653 model by (Abuel-Naga, Bergado, Bouazza, et al., 2007; Y. J. Cui et al., 2000; Hong et al.,  
 654 2013; Yao & Zhou, 2013; Zhu et al., 2021), is mentioned in eq. 8.

$$655 \quad K = \frac{(1+e)}{k} p' \quad (8)$$

656  $e$  and  $k$  is initial void ratio and elastic unloading index, respectively. Moreover, (Laloui &  
 657 François, 2009) have developed a hypo-elastic modulus for  $K$  as follows (Eq. 9).

$$658 \quad K = K_{ref} \left( \frac{p'}{p'_{ref}} \right)^{n^e} \quad (9)$$

659 Where,  $K_{ref}$  is equal to reference bulk modulus at reference pressure  $p'_{ref}$ .  $n^e$  is soil  
 660 parameter.

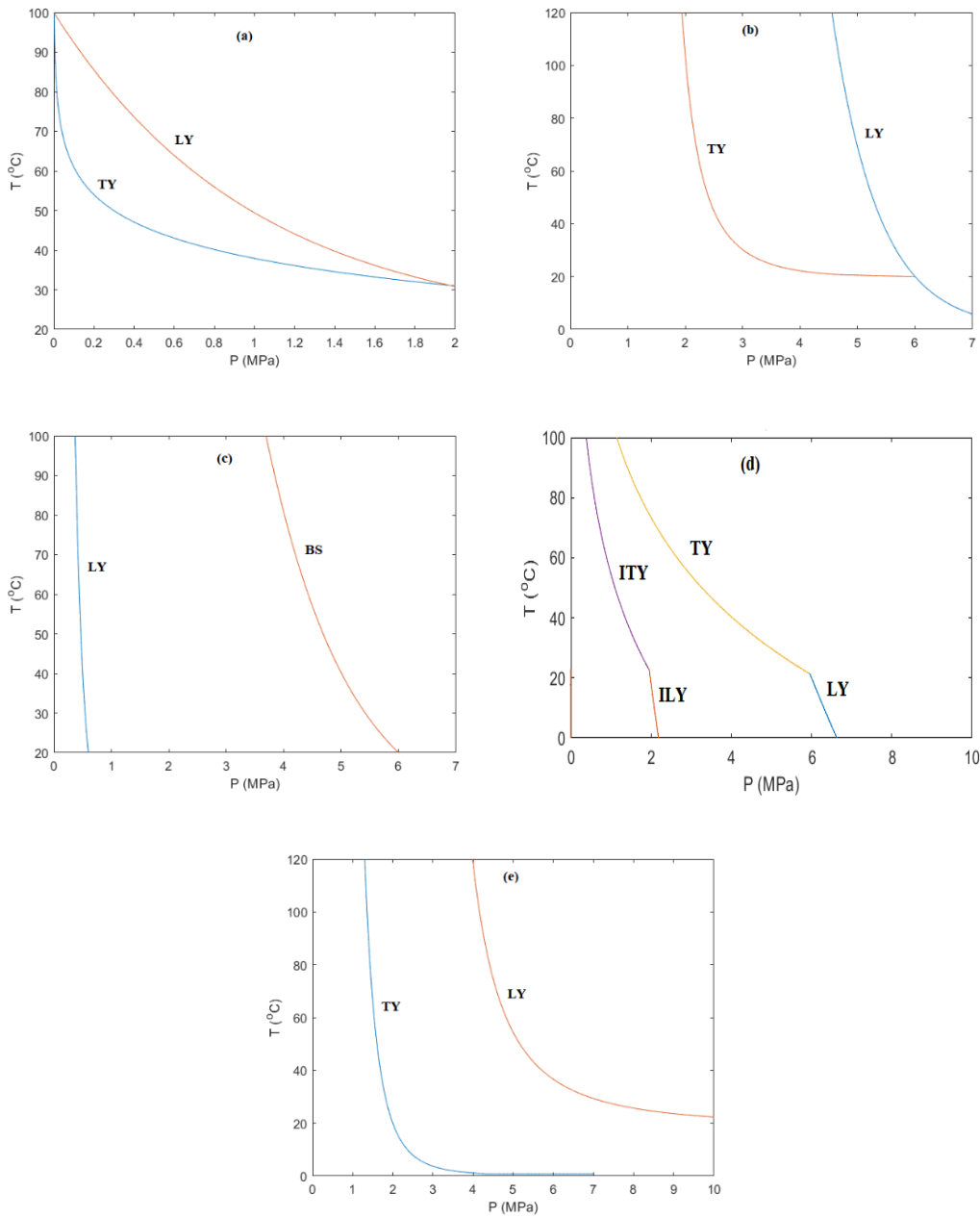
## 661 **4.2. Yield surfaces**

662 Existing thermal constitutive models can predict thermo-elasto-plastic behaviour by  
 663 adopting one or more thermal yield surfaces to define the boundary between the thermo-  
 664 mechanical elastic and plastic domains. It is more common to avail one yield surface to  
 665 observe the influence of effective stress as well as temperature changes (François & Laloui,  
 666 2008; T. Hueckel & Baldi, 1990; Laloui & François, 2009; Yao & Zhou, 2013). Likewise,  
 667 some studies have employed two yield surfaces to independently record actual temperature  
 668 and stress effects on soil (Abuel-Naga, Bergado, Bouazza, et al., 2007; Y. J. Cui et al., 2000;  
 669 Hong et al., 2016; Zhu et al., 2021). Yield locus, which is developed to enhance the  
 670 volumetric change due to effect of OCR, is called as loading yield, LY. Locus of loading



671 yield has been developed by several researchers. Thermo-mechanical yield limits for several  
 672 consecutive models are represented in fig. 13.

673



674

675

676 **Fig. 13.** Thermo-mechanical yield limits (LY and TY) for a) (Y. J. Cui et al., 2000), b)  
 677 (Abuel-Naga, Bergado, Bouazza, et al., 2007), c) (Laloui & François, 2009), d) (Hong et al.,  
 678 2016) and e) (Zhu et al., 2021)  
 679 Cui et al., (2000) have developed an equation for LY (refer fig. 13(a)), in which decrease in  
 680 pre-consolidation pressure has been observed with increasing temperature (refer Eq. 10)

681

$$p' = p_0 \exp(-\beta_0 \Delta T) \quad (10)$$

682 Where,  $p'_0$  is pre-consolidation pressure at  $T_o$  and intersection of LY curve at  $p'$ -axis.  $\beta_0$  is  
683 curvature of LY. Moreover, (Abuel-Naga, Bergado, Bouazza, et al., 2007) have also defined  
684 the LY curve in different concept. Pre-consolidation pressure is not affected during heating,  
685 however increase during cooling phase (refer fig. 13(b)). Mathematical equation is written in  
686 eq. 11.

$$687 \quad \frac{p_c(T)}{p_c(T_o)} = 1 - \gamma^{LY} \left[ \log \left( \frac{T}{T_o} \right) \right] \quad (11)$$

688  $\gamma^{LY}$  is defined as model parameter and dependent on type of soil. It is zero in heating phase  
689 and non-zero for cooling state. Laloui & François, (2009) have developed a bounding surface  
690 (BS) concept along with LY curve, as shown in fig. 13(c). LY curve is defined as to deal with  
691 both normally consolidated and over-consolidated states. The bounding surface (BS) can be  
692 used for the conventional thermo-mechanical state. The equation for LY and BS is mentioned  
693 in eq. 12 and eq. 13, respectively.

$$694 \quad \frac{p_c(T)}{r_{iso} p_c(T_o)} = 1 - r_T \left[ \log \left( \frac{T}{T_o} \right) \right] \quad (12)$$

$$695 \quad \frac{p_c(T)}{p_c(T_o)} = 1 - r_T \left[ \log \left( \frac{T}{T_o} \right) \right] \quad (13)$$

696 Where,  $r_T$  is defined as curvature of yield surface.  $r_{iso}$  is defined as the ratio of mean effective  
697 stress,  $p_c(T_o)$  at loading surface to mean effective stress at bounding surface.  $r_{iso}$  is evaluated  
698 between 0 to 1, if its value is unity then BS and LS coincide to each other. Furthermore, Yao  
699 & Zhou, (2013) have adopted similar LY curve as Cui et al., (2000) to define the thermo-  
700 elasto-plastic behaviour of soil. The equation of LY curve is adopted by (Yao & Zhou, 2013),  
701 which is written in eq. 14.

$$702 \quad p' = p'_0 \exp(-\beta \Delta T) \quad (14)$$

$$703 \quad \beta = \nu(\lambda_T - K_T)/(\lambda - K) \quad (15)$$

704 Where,  $\nu$  is defined as specific volume.  $\beta$  is written in eq. 15.  $\lambda$  and  $\lambda_T$  is referred as thermo-  
705 elasto-plastic unloading index and thermo-elasto-plastic compression index, respectively.  $K$

706 and  $K_T$  is thermo-elastic unloading index and thermo-elastic compression index, respectively.  
 707 Additionally, (Cheng et al., 2020; Hong et al., 2016) have adopted the two yield surface  
 708 approach for smooth transition from elastic to plastic state, as shown in fig. 13(d).  
 709 Conventional yield behaviour and inner yield behaviour has been introduced for LY and ILY  
 710 respectively by (Cheng et al., 2020; Hong et al., 2016), expression for LY is written in p-q-T  
 711 space in eq. 16, respectively.

$$712 \quad f_{LY} \equiv q^2 + \frac{M_f^2}{1-k_f} \left( \frac{p'}{p'_{cT}} \right)^{2/k_f} p'_{cT}{}^2 - \frac{M_f^2 p'^2}{1-k_f} = 0 \quad (16)$$

$$713 \quad \text{With, } p'_{cT} = p'_{co} \exp[-\alpha_o(T - T_o)] \quad (16a)$$

714 Where,  $M_f$  and  $k_f$  are parameter to specify the shape of LY at given temperature.  $p'_{cT}$  and  $p'_{co}$   
 715 are defined as pre-consolidation pressure at temperature T and  $T_o$ , respectively.  $\alpha_o$  controls  
 716 the curvature of LY. ILY is described as homologous to LY with respect to origin in p-q-T  
 717 space, the definition of ILY is defined in eq. 17.

$$718 \quad f_{ILY} \equiv q^2 + \frac{M_f^2}{1-k_f} \left( \frac{p'}{r^{LY} p'_{cT}} \right)^{2/k_f} (r^{LY} p'_{cT})^2 - \frac{M_f^2 p'^2}{1-k_f} = 0 \quad (17)$$

719 Where,  $r^{LY}$  is defined as a ratio of size of yield surface and corresponding inner yield surface.  
 720 Its value is always smaller than or equal to 1. Furthermore, (Zhu et al., 2021) have developed  
 721 a logarithmic equation for mechanical yield in p-q space (refer fig. 13(e)). Expression of LY  
 722 curve is written in eq. 18.

$$723 \quad \ln \left( \frac{p_c(T)}{p_c(T_o)} \right) = \theta \ln \left( \frac{T_o}{T} \right) \quad (18)$$

724 Where,  $\theta$  is soil parameter which determine the thermal dependence of preconsolidation  
 725 pressure. According to the LY yield surface, an instantaneous contraction would turn out for  
 726 normal consolidated specimen. But LY surface could not clearly define for the specimen with  
 727 higher OCR value, which undergo to expansion upon heating. Further, utilization of LY  
 728 surface may over predict the transition temperature for light to medium OCR soils.

729 To accommodate these drawbacks, a new plastic mechanism has been proposed,  
 730 which is based on a new locus yield, is called TY. This yield curve is related to the yield  
 731 curve LY, with both curves forming the boundary of the elastic region in the plane T-p'. This  
 732 mechanism allows the generation of thermoplastic deformations for over consolidated soils  
 733 exposed to heat under load. Expansion-contraction behaviour is also defined with TY surface.  
 734 It is evaluated that the sample exhibits entirely elastic deformation upon increasing the  
 735 temperature and effective stress below TY surface. Hence, increase in temperature beyond  
 736 the previous temperature imposed on soil develops the plastic strain. Cui et al., (2000) have  
 737 defined the locus of TY curve, as shown in fig. 13(a). An expression is also developed to  
 738 define the locus of TY surface, which is as follows (Eq. 19):

$$739 \quad T_{yield} = (T_c - T_0) \exp(-\beta p') + T_0. \quad (19)$$

740 Where,  $T_c$  is reference temperature at  $p' = 0$ .  $\beta$  is soil parameter to define curvature of the  
 741 curve. Similar consecutive model has been mentioned by (Abuel-Naga, Bergado, Bouazza, et  
 742 al., 2007) and (Zhu et al., 2021) in fig. 13(b) and fig. 13(e), respectively, to evaluate the TY  
 743 curve as a nonlinear function with modelling parameters in eq. 20.

$$744 \quad \frac{p_c(T_0)}{p_c(T)} = \gamma^{TY} \sqrt{\ln\left(\frac{T}{T_0}\right)} + 1 \quad (20)$$

745 Where,  $\gamma^{TY}$  is defined as shape parameter. Furthermore, the expression of TY curve, which is  
 746 developed by Cheng et al., (2020) and Peng Yun Hong et al., (2016), shows in fig. 13(d). The  
 747 mathematical equation is written in eq. 21.

$$748 \quad f_{TY} \equiv T - T_c + \frac{1}{\beta} \ln\left(\frac{p'}{p'_{ref}}\right) = 0 \quad (21)$$

749 Where,  $p'_{ref}$  is taken as reference pressure and equal to atmospheric pressure.  $T_c$  and T are  
 750 the yield temperature corresponding to  $p'_{ref}$  and  $p'$ .  $\beta$  is defined as parameter to control the  
 751 TY curve. Similar to ILY, ITY has been developed as homologous to TY curve, which is  
 752 mentioned in eq. 22.

753 
$$f_{ITY} \equiv T - r^{TY} T_c + \frac{1}{\beta} \ln \left( \frac{p'}{p'_{ref}} \right) = 0 \quad (22)$$

754 Where,  $r^{TY}$  is defined as a ratio of size of yield surface and corresponding inner yield  
 755 surface. Its value is always smaller than or equal to 1.

756 **4.3. Plastic strains**

757 A mathematical expression has been developed to predict the plastic strain with  
 758 change in temperature (Y. J. Cui et al., 2000), is as follows (Eq. 23):

759 
$$d\varepsilon_{vT}^P = \alpha_p [exp(\alpha_p \Delta T) - a] dT. \quad (23)$$

760 Where, 'a' is the shape parameter and usually near about unit.  $\alpha_p$  is slope of thermal  
 761 volumetric curve, which can be dependent on OCR. Hence, (Y. J. Cui et al., 2000) have  
 762 developed a separate equation for normal consolidation (i.e.- LY) and over consolidated (i.e.-  
 763 TY) soil in Eq. 24 and Eq. 24a, respectively.

764 
$$\alpha_p = -\frac{\alpha}{1-a} \quad (24)$$

765 
$$\alpha_p = \frac{\alpha}{exp\left(\frac{1}{c_2} \ln\left(\frac{1}{c_1} \frac{p'}{p'_0}\right)\right) - a} \quad (24a)$$

766 Where  $c_1$  and  $c_2$  are defined as parameters which can be evaluated from transition expansion  
 767 and contraction of total volumetric change due to temperature change. Moreover, (Abuel-  
 768 Naga, Bergado, Bouazza, et al., 2007) have also developed a model for thermomechanical  
 769 plastic strain due to mechanical and thermal loading, which is defined as follows (refer eq.  
 770 25)

771 
$$d\varepsilon_v^p = \frac{1}{1+e_o} \left\{ \lambda_T \frac{dp_c}{p_c} + \omega_T \frac{dp_T}{p_T} \right\} \quad (25)$$

772 Where  $\lambda_T$  and  $\omega_T$  are defined as plastic hardening modulus of LY and TY respectively.  $p_c$   
 773 and  $p_T$  are considered as mechanical and thermal pre-consolidation pressure respectively.

774 Furthermore, (Zhu et al., 2021) have described the plastic volumetric strain due to mechanical  
 775 and thermal loading. Plastic volumetric strain is mentioned below for TY and LY, in eq. 26  
 776 and eq. 27, respectively.

$$777 \quad d\varepsilon_{vTY}^p = \omega(T - T_o) \left[ \frac{p}{p_{co}} \right]^2 dT \quad (26)$$

$$778 \quad d\varepsilon_{vLY}^p = d\lambda_m \frac{\partial g^{LY}}{\partial p} \quad (27)$$

779 Where,  $d\lambda_m$  is described as a plastic multiplier, a positive value.  $g^{LY}$  is defined as a plastic  
 780 potential function as per LY. The expression of  $g^{LY}$  is written below in eq. 28.

$$781 \quad g^{LY} = k \ln \left[ 1 + (k - 1) \left( \frac{\eta}{M} \right)^2 \right] + 2(k - 1) \ln \left( \frac{p}{C} \right) \quad (28)$$

782 Where,  $\eta$  is a stress ratio ( $=q/p$ ).  $M$  is defined as slope of critical state line at  $q$ - $p$  scale.  $C$   
 783 indicates the plastic potential surface.

#### 784 **4.4.Hardening law**

785 If the stress is increased at constant temperature, or temperature is increased at  
 786 constant stress, or both stress and temperature are increased, the yield surface would  
 787 gradually approach towards the plastic zone. Further, as the yield loci move towards the right,  
 788 a hardening tendency develops which expands towards the elastic zone (Y. J. Cui et al.,  
 789 2000). The movement of LY curve has not any alteration of TY curve. Contrariwise,  
 790 influence of TY on the LY curve should be considered for the modelling of over  
 791 consolidation effect (Y. J. Cui et al., 2000; Towhata et al., 1993). When TY curve is passed  
 792 by the thermo-mechanical path, hardening phenomena has been developed and governed by  $\beta$   
 793 as a hardening parameter for TY curve. The following hardening law is defined for TY by (Y.  
 794 J. Cui et al., 2000) in eq. 29.

$$795 \quad d\beta = \frac{-\exp(\beta p')}{p'(T - T_o) \alpha_p [\exp(\alpha_p \Delta T) - a]} d\varepsilon_{vT}^p - \frac{\beta}{\alpha_1} d\varepsilon_{vTp}^p \quad (29)$$

796 Where,  $d\varepsilon_{vT}^p$  and  $d\varepsilon_{vTp}^p$  are defined as the thermal and mechanical plastic strains,  
 797 respectively, when loading path touches TY curve.  $\alpha_1$  is defined as plastic modulus.  
 798 Hardening law for LY curve has also been defined by (Y. J. Cui et al., 2000) in eq. 30, where  
 799  $p'_o$  is considered as hardening parameter.

$$800 \quad \frac{dp'_o}{p'_o} = \frac{\alpha_o}{\alpha_p[\exp(\alpha_p\Delta T)-a]} d\varepsilon_{vTp}^p + \frac{v_o}{\lambda-k} [d\varepsilon_{vp}^p + d\varepsilon_{vTp}^p] + \left\{ \frac{\alpha_o}{\alpha_p[\exp(\alpha_p\Delta T)-a]} + k \left( \frac{v_o}{\lambda-k} \right) \right\} d\varepsilon_{vT}^p \quad (30)$$

801 Where,  $\varepsilon_{vTp}^p$  and  $d\varepsilon_{vp}^p$  are referred as the thermal and mechanical plastic strain, respectively,  
 802 when loading path touches LY curve.  $k$  is defined as parameter that developed due to  
 803 coupling effect of TY and LY. The value of  $k$  depends on the magnitude of over  
 804 consolidation ratio. If  $k=0$ , no thermal hardening has been observed for NC sample.  $\alpha_o$  is a  
 805 curvature of LY curve. Moreover, (Abuel-Naga, Bergado, Bouazza, et al., 2007) have defined  
 806 a theoretical mechanism to evaluate the plastic strain along thermal loading path. Along  
 807 heating, the hardening effective stress on TY decreased with increase in temperature  
 808 according to locus of TY curve. No hardening law is developed for TY. However, hardening  
 809 law for LY is developed by (Abuel-Naga, Bergado, Bouazza, et al., 2007), which is  
 810 controlled by hardening parameter,  $p'_{co}$  (refer eq. 31).

$$811 \quad \frac{dp'_{co}}{p'_{co}} = \frac{v_o}{\lambda-k-\omega_T} d\varepsilon_{vTp}^p \quad (31)$$

812 (Laloui & François, 2009) have adopted a hardening law for TY as a function of hardening  
 813 parameter,  $r_{iso}$ .  $r_{iso}$  is governed by the consistency condition. Following expression is  
 814 considered for the loading condition, which is a hyperbolic function of plastic volumetric  
 815 strain (refer eq. 32).

$$816 \quad dr_{iso} = \frac{(1-r_{iso})^2}{c} d\varepsilon_v^p \quad (32)$$

817 For unloading condition,  $r_{iso}$  decreased to follow the decrease in mean effective stress,  $p'$ . At  
 818 reloading condition last change in direction of mean effective stress on unloading- loading,  
 819  $r_{iso}$  is adjusted to define the elastic nuclei,  $r_{iso}^e$ , which be defined in eq. 33.

820 
$$r_{iso} = r_{iso}^e + \frac{p'_{cyc}}{p'_o} \quad (33)$$

821  $p'_{cyc}$  is defined as mean effective stress at last change of direction of unloading-loading. The  
 822 hardening law for LY is defined as a relationship between volumetric plastic strain,  $\varepsilon_v^p$  and  
 823 pre-consolidation pressure,  $p'_o$  (refer eq. 34)

824 
$$dp' = \beta p'_o (d\varepsilon_v^p) \quad (34)$$

825 Where  $\beta$  can be classified as plastic compressibility modulus. Furthermore, (Yao & Zhou,  
 826 2013) have also described the hardening law, which is associated with modified cam clay  
 827 model and consider the effect of stress history. Its hardening is written in eq. 35.

828 
$$\overline{p}_x = \overline{p}_{x0} \int \frac{1+e}{\lambda-k} d\varepsilon_v^p \quad (35)$$

829 Where,  $\overline{p}_x$  is defined as the cross point between yield surface and  $p$ -axis.  $\overline{p}_{x0}$  is defined as  
 830 isotropic pre-consolidation pressure. Furthermore, (Cheng et al., 2020; Hong et al., 2016)  
 831 have developed the hardening law with parameters  $p'_{co}$  and  $r^{LY}$  for LY and ILY respectively.  
 832 Experimental evidence from (Y. J. Cui et al., 2000) shows that hardening of LY develops  
 833 when TY is activated. By the activation of LY, no hardening has been produced for TY. It is  
 834 unidirectional coupling of TY with LY. Therefore, plastic strain increment influenced with  
 835 plastic mechanism TY will also develop an increment in  $p'_{co}$ . The plastic hardening law for  
 836  $p'_{co}$  is described in eq. 36.

837 
$$dp'_{co} = \frac{v_o}{\lambda-k} p'_{co} (d\varepsilon_{vLY}^p + d\varepsilon_{vTY}^p) \quad (36)$$

838 Where,  $d\varepsilon_{vLY}^p$  and  $d\varepsilon_{vTY}^p$  is referred as plastic strain for LY and TY, respectively. To describe  
 839 the hardening law along thermomechanical loading as ILY is activated. The expression of  
 840  $r^{LY}$  is written in eq. 37.

841 
$$dr^{LY} = \frac{v_o}{\lambda-k} s_{LY} (1 - r^{LY}) (d\varepsilon_{vLY}^p + d\varepsilon_{vTY}^p + A_d d\varepsilon_{sLY}^p) \quad (37)$$

842 Where,  $s_{LY}$  is a material constant which control the rate of approaching ILY toward LY.  $A_d$  is  
 843 a parameter that control the shear plastic strain,  $d\varepsilon_{sLY}^p$  to soil hardening. Similarly, (Cheng et



844 al., 2020; Hong et al., 2016) have developed the hardening law for TY and ITY, which is  
 845 defined in eq. 38 and eq. 39 respectively.

$$846 \quad dT_c = \frac{v_o}{(\lambda-k)\alpha_o} f(OCR) d\varepsilon_{vTY}^p \quad (38)$$

$$847 \quad dr^{TY} = \frac{v_o}{(\lambda-k)\alpha_o} f(OCR) s_{TY} (1 - r^{TY}) d\varepsilon_{vTY}^p \quad (39)$$

$$848 \quad f(OCR) = 1 + s_{LY} \left( \frac{1}{r^{LY}} - 1 \right) \quad (39a)$$

849 Where,  $s_{TY}$  is defined as material constant that control the rate of approaching ITY to TY.  
 850 Similar to  $r^{LY}$ , contribution to  $r^{TY}$  can be used to predict the smooth elastoplastic transition  
 851 when ITY is activated. Recently, (Zhu et al., 2021) have described the hardening law by  
 852 coupling mechanical and thermal plastic mechanism, which is appeared in LY and TY  
 853 function both as a hardening parameter. The mechanical and thermal volumetric strain move  
 854 the LY and TY limit simultaneously; the hardening law is written as follow (refer eq. 40).

$$855 \quad dp_c = p_{co} \frac{1+e}{\lambda-k} (d\varepsilon_{vLY}^p + d\varepsilon_{vTY}^p) \quad (40)$$

856 Several thermo-mechanical models are discussed to evaluate the elastic and plastic  
 857 volumetric strain due to thermal and mechanical loading. (Abuel-Naga, Bergado, Bouazza, et  
 858 al., 2007; Cheng et al., 2020; Y. J. Cui et al., 2000; Hong et al., 2016; Zhu et al., 2021) have  
 859 introduced the two-yield surface to describe the thermo-mechanical plastic strain. Meanwhile,  
 860 (Laloui & François, 2009; Yao & Zhou, 2013) have adopted single yield surface mechanism.  
 861 For better understanding, TY and LY is coupled to determine the plastic strain through the  
 862 change in size of yield surface. It can be demonstrated that many thermo-mechanical features  
 863 such as thermal volumetric strain of soil at different OCR and thermally induced strength of  
 864 soil are well described with constitutive model.

#### 865 **4.5.Heating under undrained conditions**

866 The method for prediction of excess pore pressure due to undrained heating response  
 867 has been described in numerous literatures (Abuel-Naga, Bergado, & Bouazza, 2007;

868 Burghignoli et al., 2000; Campanella & Mitchell, 1968; Ghaaowd et al., 2015; Houston et al.,  
869 1985; Mohajerani et al., 2012; Salager et al., 2008; Uchaipichat & Khalili, 2009). These  
870 studies have indicated that the initial void ratio, effective stress, stress history and change in  
871 temperature can affect the magnitude of excess pore pressure. (Mohajerani et al., 2012)  
872 observed that in undrained thermo-mechanical study, pore pressure increased in porous  
873 material in following manner (Eq. 41).

$$874 \quad \Delta u = B\Delta\sigma + \Lambda\Delta T \quad (41)$$

875 Where,  $B$  and  $\Lambda$  are described as Skempton coefficient and thermal pressurization coefficient.  
876 In this context, Ghaaowd et al., (2015) have illustrated while performing heating test without  
877 drainage that, the water pressure in the pores increased linearly with temperature. Moreover,  
878 over-consolidation ratio alters the pore pressure in a way that as OCR value increases while  
879 pore water pressure decreases for a particular temperature (Abuel-Naga et al., 2007a;  
880 Uchaipichat and Khalili, 2009; Ghaaowd et al., 2015). A theoretical formula has also been  
881 established to estimate the pore pressure for saturated soil without drainage during heating  
882 cycles by utilizing the thermo-elastic and linear elastic concept in Eq. 42 (Campanella and  
883 Mitchell, 1968). The theoretical formula is written as follows:

$$884 \quad \Delta u = \frac{\eta\Delta T (\alpha_s - \alpha_w) + \alpha_{st}\Delta T}{m_v} \quad (42)$$

885 Where,  $\alpha_{st}$  is coefficient of structural volume change.  $\alpha_s$  and  $\alpha_w$  are the coefficient of thermal  
886 expansion for soil solids and pore water, respectively. The value of  $\alpha_s$  and  $\alpha_w$  were reported  
887 by researchers such as equal to  $0.000035/^\circ\text{C}$  and  $0.00017/^\circ\text{C}$  (Campanella and Mitchell, 1968;  
888 Burghignoli et al., 2000), whereas the reported value of  $\alpha_{st}$  is  $-0.00005/^\circ\text{C}$  (Mitchell and Soga,  
889 2005). Further, Campanella and Mitchell, (1968) did not consider the effect of plasticity  
890 index, PI, so the effect of average PI was consider to plot the curve for  $\alpha_{st}$ . Although, it has  
891 been conveyed with some scatter that the value of  $\alpha_{st}$  decreases non-linearly with increase in

892 plasticity index of specimen (Mitchell and Soga, 2005). Additionally, an relationship between  
 893  $\alpha_{st}$  and PI has been derived by Ghaaowd et al., (2015) and the same is expressed in Eq. 43:

$$894 \quad \alpha_{st} = 1 \times 10^{-4} e^{-0.014PI}. \quad (43)$$

895         Nonetheless, the above investigation has recommended that extensive studies should  
 896 be carried out on different soil type, so that a better relationship between  $\alpha_{st}$  and  $PI$  can be  
 897 obtained. It is accepted that such development of the Eq. 43 will facilitate quick and accurate  
 898 determination of  $\Delta u$  without resorting to detailed test reports. Furthermore, it has been stated  
 899 that the pore water pressure of saturated soil is effected by the stress history (OCR) at  
 900 different temperature (Abuel-Naga et al., 2007a) . It has been reported that the pore water  
 901 pressure decreases with increase in OCR. Similar trend has been observed by (Ghaaowd et  
 902 al., 2015). Subsequently, thermally induced pore water pressure is observed as reversible for  
 903 NC soil and it is irreversible for OC soil, that also generates negative pore pressure while  
 904 cooling to room temperature (Hueckel and Pellegrini, 1992; Abuel-Naga et al., 2007a).  
 905 However, thermal induced pore water pressure for unsaturated soil has not been explored  
 906 significantly.

#### 907 **4.6.Creep behaviour**

908         Several researchers have proposed the equation to bridge the creep coefficient and  
 909 temperature (Fox & Edil, 1996; Houston et al., 1985; Zhu & Qi, 2018). Regarding this, Zhu  
 910 and Qi, (2018) have adopted an elastic visco-plastic model, in which temperature dependent  
 911 creep against one dimensional loading is described and the results were compared vis-à-vis  
 912 with the results obtained from experimental investigation. For visco-plastic strain ( $\epsilon_v^{vP}$ ), 1-D  
 913 model proposed by Kutter & Sathialingam, (1992), which is based on creep coefficient,  $\psi_T$   
 914 (refer eq. 44).

$$915 \quad \epsilon_v^{vP} = \frac{\psi_T}{(1+e_o)t_r} \left( \frac{\sigma_v}{\sigma_v^r} \right)^{\lambda-k/\psi_T} \quad (44)$$

916 Where,  $e_o$  is initial void ratio.  $t_r$  is defined as a reference time and equal to time taken in  
 917 each load increment.  $\sigma_v$  is effective vertical stress.  $\sigma_v^r$  is reference stress corresponding to  
 918 load increment time,  $t_r$ .  $\lambda$  and  $k$  is referred as slope of compression line and recompression  
 919 line respectively. It has been reported that the secondary thermal consolidation initiates  
 920 taking place after completion of dissipation of pore water, and the induced settlement occurs  
 921 due to the effect of time and temperature. Thus, coefficient of thermal creep is defined as the  
 922 slope of thermal secondary consolidation curve, given in void ratio and time in log scale (e vs  
 923 log (t)) (Zhu and Qi, 2018). Moreover, linear function is derived between thermal creep  
 924 coefficient and temperature (Houston et al., 1985), which is written (eq. 45),

$$925 \quad \psi_T = A \times T. \quad (45)$$

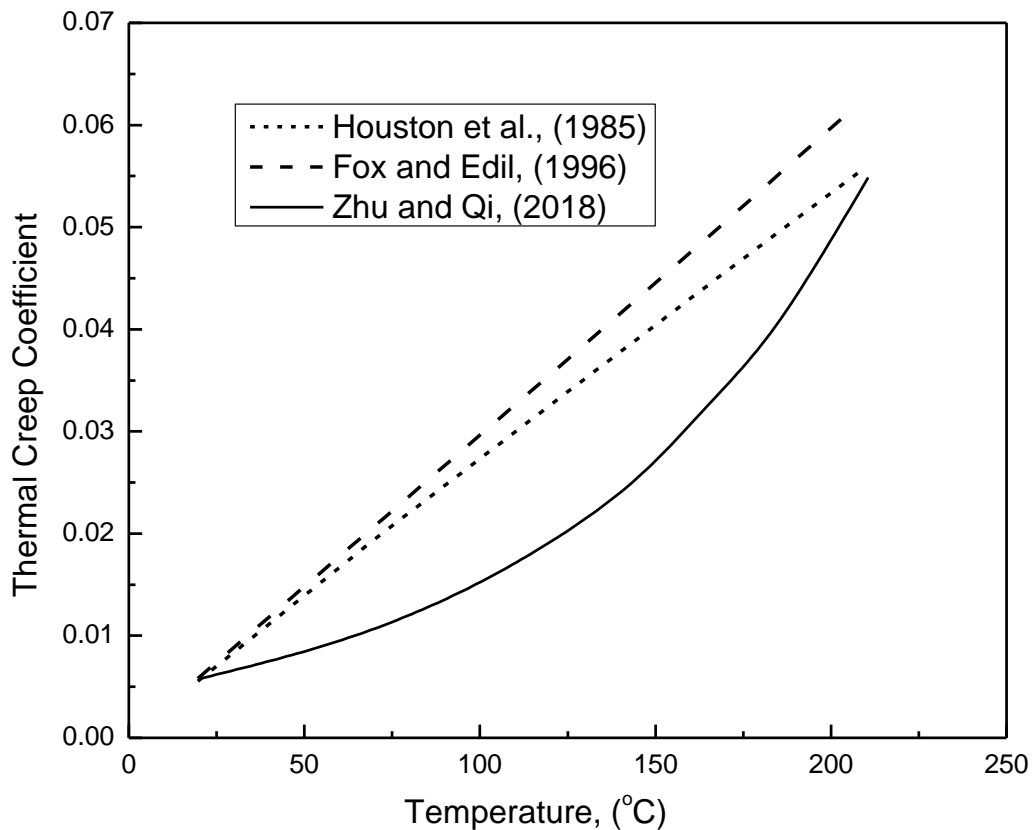
926 Where,  $\psi_T$  is thermal creep coefficient under specific temperature ‘T’ and A is  
 927 thermal parameter. The value of A has been considered as 0.0105 (Houston et al., 1985) and  
 928 it was stated that ‘ $\psi_T$ ’ linearly increases with temperature. Hence,  $\psi_T$  will be zero and  
 929 negative when the corresponding temperature is zero and negative respectively. On the  
 930 contrary, another equation has been represented based on the experimental study for  
 931 development of ‘ $\psi_T$ ’ with change in temperature (Fox and Edil, 1996), which is mentioned  
 932 below (Eq. 46):

$$933 \quad \psi_T = \psi_{Tr} \exp [B (T-T_r)]. \quad (46)$$

934 Where,  $\psi_{Tr}$  is reference thermal creep coefficient for reference temperature ‘ $T_r$ ’ and B is  
 935 thermal parameter, whose value is equal to  $0.25 \pm 0.02/^\circ\text{C}$  (Fox and Edil, 1996). However, at  
 936 a higher temperature, the value of  $\psi_T$  crosses beyond the normal range as per eq. 46.  
 937 Additionally, (Zhu and Qi, 2018) have also noticed a nonlinear increment in thermal creep  
 938 coefficient with increase in temperature, which can be written as (Eq. 47):

$$939 \quad \psi_T = \psi_{Tr} \left( \frac{T}{T_r} \right)^{C_T}. \quad (47)$$

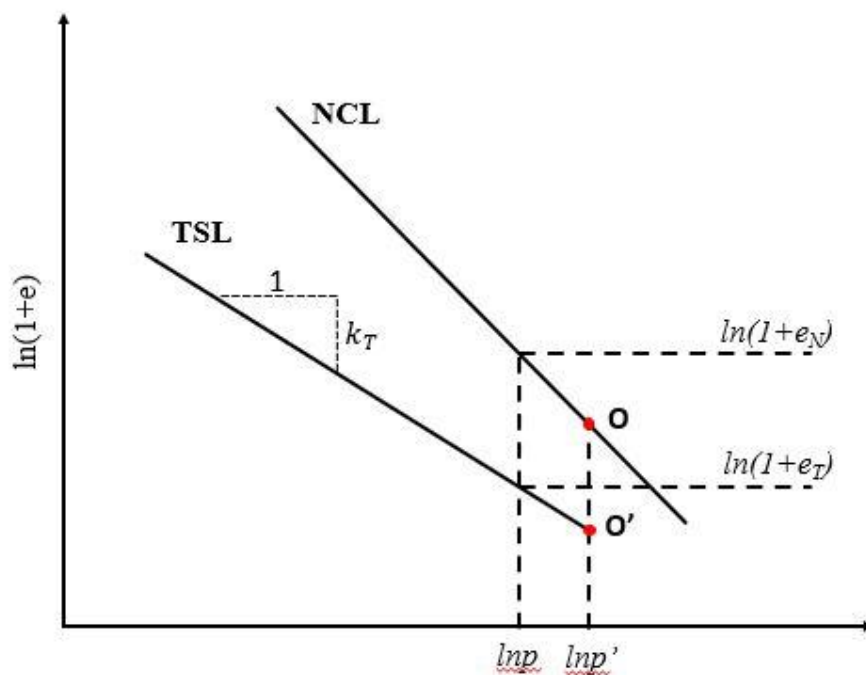
940 Where,  $C_T$  is thermal related parameter. Based on the experimental results the value  
 941 of  $C_T$  was considered as 0.95 (Zhu and Qi, 2018). It is worthwhile to mention that eq. 47  
 942 resolves the limitation associated with Eq. 45 and eq. 46 in terms of minimum and maximum  
 943 value of thermal creep coefficient. Hence, fig. 14 developed by comparison among eq. 45, eq.  
 944 46 and eq. 47, which describing the relation between thermal creep coefficient with  
 945 temperature. However, the effect of temperature on creep behaviour of soil was illustrated  
 946 experimentally (Jarad et al., 2019; Zhu et al., 2017; Zhu & Qi, 2018) but needs a clear  
 947 representation. Moreover, a 1-D direct modelling of thermal creep is developed by (Zhu &  
 948 Qi, 2018), which is elastic-visco-plastic (EVP) model. This model is developed to assume  
 949 that the loading condition is one dimensional and limited to soft clay. Hence, a particular  
 950 model which replicates the real time loading pattern for soils needs to be developed.



951 **Fig. 14.** Relationship of thermal creep coefficient with temperature from eq. (42), (43) and  
 952 (44).  
 953

954 **4.7. Modelling of volumetric change under temperature cycle**

955 As obtained from experimental results, a thermal stabilisation line has been proposed,  
 956 which controls the stabilized soil against the cyclic temperature loading (Campanella &  
 957 Mitchell, 1968; Di Donna & Laloui, 2015; Vega & McCartney, 2014). As shown in fig. 15,  
 958 the normal compression line (NCL) and the thermal stabilization line (TSL) at elevated  
 959 temperature is assumed to be a straight line in  $\ln v - \ln p'$ . Where, the point O refers to the state  
 960 of NC soil for first heating cycle. Similarly, point O' represents the stabilized soil after  
 961 several temperature cycle with given temperature increase. The distance between OO'  
 962 represents the irreversible volumetric contraction of NC soil with respect to first cyclic  
 963 heating. If point O and O' coincides then it is said that no accumulation of irreversible  
 964 volumetric compression occurs. Therefore, it can be opined that as temperature changes, the  
 965 TSL and NCL shifts together, which also reflect from experimental results by Campanella &  
 966 Mitchell, (1968). During heating, if soil state lies above TSL then irreversible volumetric  
 967 compression develops, otherwise the response is elastic in nature. While cooling, reversible  
 968 volumetric change develops (Ma et al., 2017).



969  
 970

**Fig. 15.** Proposed Model Line for TSL (Q. J. Ma et al., 2017).

971 Hence, it is very difficult to quantify the effect of temperature on TSL experimentally. As  
 972 stated by Ma et al., (2017), the accumulation and stabilization of irreversible volumetric  
 973 compression along temperature cycles can be well defined by thermal shakedown. According  
 974 to concept of thermal shakedown, the soil sample reaches the stabilized state after certain  
 975 temperature cycle. For mechanical loading, volumetric change of specimen is equivalent to  
 976 change in void ratio. However, during thermal loading volume change of specimen is due to  
 977 deformation of soil void as well as soil particles, which is reversible in nature during cooling.  
 978 Therefore, NCL and TSL return to its initial position during cooling for first thermal cycle.  
 979 (Ma et al., 2017; Mašin & Khalili, 2012). TSL and NCL moves down with increase in  
 980 temperature. TSL shifts more as compared to NCL. Furthermore, after several temperature  
 981 cycle, soil state reaches the TSL with elevated temperature and vertical distance becomes  
 982 zero. So there is no irreversible amount of compression if the temperature does not exceed the  
 983 maximum value of the previous heating. Mašin & Khalili, (2012) have developed an  
 984 expression for temperature dependent NCL, which is written following (Eq. 48):

$$985 \quad \ln(1 + e) = N(T) - \lambda(T) * \ln(\sigma' / \sigma_r) \quad (48)$$

986 Where,  $e$  is void ratio;  $\sigma'$  is mean effective stress;  $\sigma_r$  is reference stress (1kPa).  $\lambda(T)$  and  
 987  $N(T)$  are defined as temperature dependent slope and intercept of NCL, respectively, which is  
 988 expressed in eq. 49 and eq. 49a:

$$989 \quad \lambda(T) = \lambda(T_r) + l_T * \ln\left(\frac{T}{T_r}\right) \quad (49)$$

$$990 \quad N(T) = N(T_r) + n_T * \ln\left(\frac{T}{T_r}\right) \quad (49a)$$

991 Where,  $l_T$  and  $n_T$  are the modelling parameters which controls the change of slope and shifts  
 992 of NCL, respectively.  $T_r$  is the reference temperature. From the experimental results, it can be  
 993 concluded that  $\lambda$  is independent of temperature (Campanella & Mitchell, 1968). Therefore,  $l_T$

994 should be taken as zero. Similarly, an expression has been developed to introduce TSL with  
 995 respect to temperature, which is written below in eq. 50 (Ma et al., 2017):

$$996 \quad \ln(1 + e) = \ln(1 + e') - k_T * \ln(p/p') \quad (50)$$

997 Where,  $p'$  is termed as pre-consolidation pressure. Therefore, Ma et al., (2017) have  
 998 developed another equation to calculate  $\ln(1 + e')$ , which is mentioned in eq. 51:

$$999 \quad \ln(1 + e') = \ln(1 + e_o) + c_T * n_T * \ln(T/T_r) \quad (51)$$

1000 Where  $e_o$  &  $e'$  is defined as void ratio for point O & O', respectively. Here, it is assumed that  
 1001 if temperature is less than reference temperature then  $e'$  is equal to  $e_o$ . Moreover,  $c_T$  is used  
 1002 to determine the accumulated volumetric compression after the first thermal cycle. If there is  
 1003 no accumulation, then  $c_T$  is equal to zero.  $k_T$  is slope parameter which is used to simulate the  
 1004 irreversible volumetric contraction of soil. As mentioned,  $k_T$  is inversely proportional to  
 1005 irreversible volumetric contraction. If  $k_T$  decreases, simulated irreversible volumetric  
 1006 contraction increases for soil. Di Donna & Laloui, (2015) have developed a bounding surface  
 1007 to reproduce the response of soil under thermal cyclic loading. This model can able to show  
 1008 the behaviour of soil beyond the thermo-elastic and thermo-plastic behaviour depending upon  
 1009 the soil stress state and accumulation phenomena. Therefore, isotropic yield mechanism,  $r_{iso}$   
 1010 is developed to re-initialisation of locus at which plasticity starts during next heating phase  
 1011 (in Eq. 52).

$$1012 \quad r_{iso} = r_{iso}^{cyc} + \frac{p'}{p'_c} \quad (52)$$

1013 Where,  $r_{iso}^{cyc}$  is defined as material parameter that depends to accumulate plastic deformation  
 1014 during thermal cycle. When heating restarts,  $r_{iso}$  is constant till the re-initialised yield surface  
 1015 is achieved. Therefore, during re-heating plasticity again started at temperature  $T^*$  that define  
 1016 as a following equation 53.

$$1017 \quad p' - p'_o e^{\beta \varepsilon_v^p} \left[ 1 - \gamma_T \cdot \ln\left(\frac{T^*}{T_o}\right) \right] \left( r_{iso}^{cyc} + \frac{p'}{p'_o e^{\beta \varepsilon_v^p}} \right) \quad (53)$$



1018 Furthermore, (Zhou et al., 2017) have purposed a two boundary surface to capture the effect  
 1019 of thermal cycle. The original bounding surface was modified with two bounding surface (i.e.  
 1020 - a bounding surface and a memory surface). The bounding surface,  $F$  is expressed in the  
 1021 following expression (refer eq. 54):

$$1022 \quad F = \left(\frac{q}{Mp'}\right)^n + \frac{\ln(p'/p_o)}{\ln r} \quad (54)$$

1023 Where,  $n$  and  $r$  is the soil parameter, which controls the shape of bounding surface.  $M$  is the  
 1024 value of critical state stress ratio. Moreover, the memory surface,  $F^*$  can be expressed as a  
 1025 following equation 55:

$$1026 \quad F^* = \left(\frac{q}{Mp'}\right)^n + \frac{\ln(p'/p_l)}{\ln r} \quad (55)$$

1027 Where,  $p_l$  can be described as the size of the loading surface. Pre-consolidation pressure,  
 1028 which is a function of plastic volumetric strain, and maximal stress state, respectively, control  
 1029 the boundary surface and memory surface. The double surface idea effectively captures  
 1030 thermal cyclic effects because the two surfaces have separate hardening laws. The  
 1031 consistency of measured and estimated soil volume changes during temperature cycles is  
 1032 demonstrated. Furthermore, Golchin et al., (2022b) have established a kinematic rule to  
 1033 measure the progressive volumetric strain of soil under thermal cycles. The inner yield  
 1034 surface, which is controlled by a kinematic rule, begins to translate when plastic strain  
 1035 increments are developed. The kinematic rule was activated during heating phase and  
 1036 deactivated during cooling phase. Therefore, the plastic volumetric strain increments  
 1037 produced and were defined in the eq. 56 (Golchin et al., 2022b).

$$1038 \quad \varepsilon_v^p = \left(\frac{1+e_o}{\lambda-k}\right)^{-1} \{\mu\langle T' \rangle + \mu\langle T - T_o \rangle\} \quad (56)$$

1039 Where,  $\varepsilon_v^p$  is defined as plastic volumetric strain increment.  $\lambda$  and  $k$  are defined as  
 1040 elastoplastic compression index and elastic compression index, respectively.  $T$ ,  $T'$  and  $T_o$   
 1041 represent the absolute temperature, temperature increment and initial temperature,

1042 correspondingly.  $\mu$  shows the coefficient of thermal softening of inner yield surface. Further,  
1043  $\langle \cdot \rangle$  is defined as Macaulay bracket, which operates as  $\langle x \rangle = (x + |x|)/2$ . This model leads to  
1044 the prediction of plastic strains in highly over-consolidated states as well as during the  
1045 heating phase of cyclic thermal loads. As the soil becomes over-consolidated and the model  
1046 has control over the accumulated plastic strains brought on by thermal loads, the magnitude  
1047 of thermally-induced plastic strains decreases on subsequent thermal cycles.

#### 1048 **4.8. Thermodynamics Model**

1049 In this section, granular thermodynamics model is used to build a new approach towards  
1050 THM mechanism. This model takes into account influencing elements such temperature,  
1051 saturation, the solid skeleton's microstructure, and phase transitions between the liquid and  
1052 solid/gas phases. The proposed conceptual model has universal physical significance because  
1053 it is supported by common experimental findings. In recent years, emphasis has been placed  
1054 on nonlinear thermodynamic constitutive models developed through the so-called  
1055 deformation work that closely adhere to the principle of energy conservation. The product of  
1056 each phase stress and the accompanying generalised strain is exactly what makes up the  
1057 deformation work. Changes in water content, soil deformation, and microstructures all have  
1058 an impact on one another. Solid, liquid, and gas phases all undergo mutual transformation,  
1059 therefore the deformation work brought on by phase transitions must also be taken into  
1060 account (Bai, Zhou, et al., 2021; Liu & Lai, 2020). Several researchers have been  
1061 implemented the thermodynamic momentum conservation law to understand the thermo-  
1062 mechanical behaviour of fine grained soil (Bai, Zhou, et al., 2021; Zhang & Cheng, 2017).  
1063 Particle temperature is the thermodynamic observable variable entropy of particles, which is  
1064 comparable to the relationship between thermodynamic temperature and entropy at the  
1065 macroscopic level. In terms of energy dissipation, this description is consistent with classical  
1066 thermodynamics, which uses entropy or temperature to denote the random motion of

1067 materials. Thus, the rearrangement of particles can reflect the plastic deformation of fine  
 1068 grained soil, which is released at this kinetic energy, can be transformed into molecular  
 1069 motion, accompanied by the production of entropy. Based on this concept, Zhang & Cheng,  
 1070 (2017) have developed a model to evaluate the mean effective stress according to  
 1071 thermodynamic law in drained condition (refer eq. 57).

$$1072 \quad p' = 1.5B(\varepsilon_v^e + c)^{0.5}[0.4(\varepsilon_v^e)^2 + \zeta(\varepsilon_d^e)^2] + 0.8B(\varepsilon_v^e + c)^{1.5}\varepsilon_v^e + K_e\beta_T(T - T_r) \quad (57)$$

1073 Where,  $\varepsilon_v^e$  and  $\varepsilon_d^e$  is volumetric elastic strain and deviatoric elastic strain, respectively. B and  
 1074  $\zeta$  is defined as the material parameter.  $K_e$  is defined as secant elastic modulus of soil.  $\beta_T$  is  
 1075 thermo-elastic volumetric coefficient of expansion of soil.  $T_r$  is reference temperature in  
 1076 kelvin. c is a parameter for allowable maximum volumetric tensile strain (i.e.-  $\varepsilon_v^e \leq c$ ).  
 1077 Similarly, Bai et al., (2019a) have also developed a model based on conservation of energy  
 1078 for mean effective stress, which is written in eq. 58:

$$1079 \quad p' = B[(\varepsilon_v^e + \beta_T\Delta T)^{0.5} + 0.5\zeta(\varepsilon_v^e + \beta_T\Delta T + c)^{-0.5}(\varepsilon_s^e)^2] + sS_r \quad (58)$$

1080 Where, s is defined as the metric suction.  $S_r$  is representing the rate of dissipative flow.  $\varepsilon_s^e$  is  
 1081 defined as second elastic strain.

## 1082 **5. Discussion**

1083 This section highlights the issues, which arises due to application of the thermal  
 1084 loading in fine-grained soil. Generally, the major issue is associated with the volumetric  
 1085 change due to the application of temperature. In this context, there are numerous independent  
 1086 literatures have been reported in this paper to mention the thermo-mechanical behavior of  
 1087 fine-grained soil. Nonetheless, there are still many studies whose observations and  
 1088 discussions are conflicting to each other against thermal volumetric change, swelling pressure  
 1089 and shear strength of soil. There are mainly two major states (macroscopic and microscopic),  
 1090 which has been considered to understand the thermally induced volumetric change of fine-  
 1091 grained soil. A considerable number of studies are available against the volumetric change of

1092 soil at macroscopic scale. However, there is few consecutive models available to describe the  
1093 direct method to identify the creep behavior, but still need to be clearly describe the creep  
1094 behavior of soil and coupled it with several parameters of soil. The available literatures also  
1095 need to describe the magnitude of primary and secondary consolidation of thermally induced  
1096 volumetric change. Moreover, there are separate experimental investigations for over  
1097 consolidation ratios and secondary compression index. Hence, these studies should be  
1098 coupled with each other for better understanding, which would also help to develop a  
1099 constitutive model regarding thermal volumetric change due to OCR and secondary  
1100 compression index. Furthermore, the speculation of thermally induced volumetric change at  
1101 microscopic scale are very limited. At microscopic level, it is very difficult to disintegrate the  
1102 bond stress between particles, degradation of adsorbed water and development of  
1103 intermolecular forces. The experimental investigation is very difficult to achieve for such  
1104 type of problems. Hence, there is an opportunity to push the knowledge boundaries and  
1105 develop a numerical model to illustrate these problems. Additionally, soil is inorganic in  
1106 nature and several inorganic minerals are present in it. Therefore, experimental investigation  
1107 remains elusive to evaluate the differential expansion of minerals upon heating. Still, there is  
1108 an opportunity to illustrate the thermally induced volumetric change with respect to the  
1109 differential thermal expansion of minerals of soil. Apart from that, there are still few  
1110 parameters such as swelling pressure due to concentration of available cations, generation of  
1111 pore water pressure with unsaturated soil and shear strength parameters of soil due to  
1112 application of temperature which needs to be discussed clearly. For the fine-grained soil,  
1113 there is no standard procedure for rate of heating, which can affect the thermal volumetric  
1114 change. On the other hand, there are still few problems (i.e., - volume change due to cyclic  
1115 thermal load, pore water pressure and shear strength parameter) which is unanswered in  
1116 literatures available for the unsaturated soil. Further investigation and constitutive models

1117 should be conducted for the better understanding of some contrasting phenomena related to  
1118 couple thermal and mechanical stress regarding microscopic behavior and mechanism.

## 1119 **6. Concluding Remark**

1120 In this article, a comprehensive review of the available literature on temperature  
1121 induced volumetric deformation of saturated and unsaturated, fine-grained soils has been  
1122 analysed thoroughly. Several parameters such as volumetric change, measurement of  
1123 swelling pressure, change in consolidation parameters and thermal elasto-plastic behaviour of  
1124 fine-grained soil specimen have been evaluated, which can get effected by the alteration in  
1125 temperature. Moreover, the mechanisms behind the thermal volumetric deformation  
1126 behaviour of the soils have also been explained in terms of alteration of the abovementioned  
1127 parameters. Among these parameters, thermo-elasto-plastic analysis has gained immense  
1128 popularity among the researchers. Additionally, it has been explained that the response of the  
1129 soils in terms of the thermal volume change behaviour has substantial influence on the initial  
1130 over-consolidation ratio. The following major conclusions are yielded from the available  
1131 literature regarding thermal volumetric change of fined grained soil:

- 1132 • The basic mechanism of the thermal volumetric change has been studied from literature  
1133 and which are 1) difference in thermal coefficient of soil solid and pore water, 2) weak  
1134 shearing bond between soil particles, 3) decrease in viscosity of pore water at high  
1135 temperature and 4) clay water interaction against thermal loading at microscopic level.
- 1136 • The thermal volumetric change behaviour typically depends on the effective stress  
1137 applied on the soil sample prior to heating. Matric suction and temperature cycle can also  
1138 alter the thermal volumetric change behaviour. Besides, it has been elucidated that the  
1139 thermal drained heating response of soil in terms expansion and contraction occur for  
1140 high and low OCR values, correspondingly.

- 1141 • The volumetric change of the soil mass due to thermal energy is independent of thermal  
1142 history i.e., imposed as temperature cycle and experienced by specimen at different  
1143 effective stress, nonetheless it can aid to enhance the stiffness and hardness of soils.
- 1144 • Nonetheless, some parameters such as intrinsic permeability and coefficient of volume  
1145 compressibility have no repercussion of temperature. These parameters are dependent of  
1146 stress magnitude instead.
- 1147 • Shear strength of soil under elevated temperature remains a contradictory matter; more  
1148 laboratory investigation is required to clarify the thermal effect of soil on shear strength.
- 1149 • The thermal loading has significant influence on creep index of specimen. Creep  
1150 Coefficient of soil is proportional to temperature and increase with increase in  
1151 temperature.
- 1152 • Several parameters such as permeability, Creep index, pore water pressure and coefficient  
1153 of consolidation is directly proportional to temperature. Whereas viscosity of pore water  
1154 is inversely proportional to induced temperature.
- 1155 • Moreover, the thermo-mechanical model including elastic and plastic strain is studied to  
1156 understand the volumetric change of soil from various available literature. Especially,  
1157 some researchers have described an alternative approach to understand the volumetric  
1158 change due to thermal secondary compression and developed the relevant mathematical  
1159 expressions. The experimental results have been utilized to validate the mathematical  
1160 models.
- 1161 • Furthermore, The Yield surface has also been defined to plot a distinct boundary between  
1162 thermo-elastic region and thermo-elasto-plastic region from temperature versus pre-  
1163 consolidation pressure plot. Different yield surfaces such as loading yield and thermal  
1164 yield surface have been defined to measure elastic and plastic volumetric change.

- 1165 • Mathematical modelling regarding creep behaviour and volumetric change under  
1166 temperature cycle has also been reported.
- 1167 • Thermodynamic modelling has also been discussed to evaluate the preconsolidation  
1168 pressure of fine grained soil using energy conservation and phase transformation.

1169 The temperature induced volumetric deformation analysis of fine-grained soil  
1170 reviewed in this study is reported mainly through laboratory experiments. It can be seen that  
1171 laboratory experiments are usually carried out in a controlled environment condition, which  
1172 in many cases could not be possible to replicate in a field scenario. Consequently, real-time  
1173 thermal volumetric deformation analysis can be affected by harsh environmental conditions  
1174 and climate change, which may or may not be possible on a laboratory scale. However, it  
1175 should be appreciated that large scale studies and their interpretation are carried out in  
1176 ongoing research and can assist in decision making by the radioactive waste management  
1177 authority, in developing holistic solutions for researchers and in identifying unforeseen  
1178 problems events to be found in the future.

1179 **CRedit authorship contribution statement**

1180 **Md Azhar:** Conceptualisation, Methodology, Formal analysis, Investigation, Writing-  
1181 original draft, Writing- review and editing, Visualisation. **Somenath Mondal:**  
1182 Conceptualisation, Methodology, Writing- review and editing, Visualisation, Supervision.  
1183 **Anh Minh Tang:** Conceptualisation, Methodology, Writing- review and editing,  
1184 Visualisation, Supervision. **Akhileshwar Kumar Singh:** Supervision.

1185 **Declaration of competing Interest**

1186 On behalf of all the authors of the submission, I declare that there are no conflicts of  
1187 interests involved in this study.

1188 **Data availability**

1189 All data and models generated or used during the study appear in the submitted  
1190 article.

### 1191 **Acknowledgment**

1192 The authors sincerely acknowledge the financial support provided by the Science and  
1193 Engineering Research Board (SERB), Government of India in the form of Start-up Research  
1194 Grant (SRG/2020/000167) at the Department of Civil Engineering, NIT Jamshedpur. In  
1195 addition, the authors also wish to thank the department of civil engineering, NIT Jamshedpur  
1196 for its immense help and guidance during the course of the study.

### 1197 **References**

- 1198 Abuel-Naga, H. M., Bergado, D. T., & Bouazza, A. (2007). Thermally induced volume  
1199 change and excess pore water pressure of soft Bangkok clay. *Engineering Geology*,  
1200 89(1–2), 144–154.
- 1201 Abuel-Naga, H. M., Bergado, D. T., & Bouazza, A. (2008). Thermal conductivity evolution  
1202 of saturated clay under consolidation process. *International Journal of Geomechanics*,  
1203 8(2), 114–122.
- 1204 Abuel-Naga, H. M., Bergado, D. T., Bouazza, A., & Ramana, G. V. (2007). Volume change  
1205 behaviour of saturated clays under drained heating conditions: experimental results and  
1206 constitutive modeling. *Canadian Geotechnical Journal*, 44(8), 942–956.
- 1207 Abuel-Naga, H. M., Bergado, D. T., & Lim, B. F. (2007). Effect of temperature on shear  
1208 strength and yielding behavior of soft Bangkok clay. *Soils and Foundations*, 47(3), 423–  
1209 436.
- 1210 Abuel-Naga, H. M., Bergado, D. T., Ramana, G. V., Grino, L., Rujivipat, P., & Thet, Y.  
1211 (2006). Experimental evaluation of engineering behavior of soft Bangkok clay under  
1212 elevated temperature. *Journal of Geotechnical and Geoenvironmental Engineering*,  
1213 132(7), 902–910.



- 1214 Alsherif, N. A., & McCartney, J. S. (2015). Nonisothermal behavior of compacted silt at low  
1215 degrees of saturation. *Géotechnique*, 65(9), 703–716.
- 1216 Bag, R., & Rabbani, A. (2017). Effect of temperature on swelling pressure and  
1217 compressibility characteristics of soil. *Applied Clay Science*, 136, 1–7.
- 1218 Bai, B., Nie, Q., Zhang, Y., Wang, X., & Hu, W. (2021). Cotransport of heavy metals and  
1219 SiO<sub>2</sub> particles at different temperatures by seepage. *Journal of Hydrology*, 597, 125771.  
1220 <https://doi.org/10.1016/j.jhydrol.2020.125771>
- 1221 Bai, B., & Shi, X. (2017). Experimental study on the consolidation of saturated silty clay  
1222 subjected to cyclic thermal loading. *Geomechanics and Engineering*, 12(4), 707–721.
- 1223 Bai, B., Yang, G., Li, T., & Yang, G. (2019a). A thermodynamic constitutive model with  
1224 temperature effect based on particle rearrangement for geomaterials. *Mechanics of*  
1225 *Materials*, 139, 103180. <https://doi.org/10.1016/j.mechmat.2019.103180>
- 1226 Bai, B., Yang, G., Li, T., & Yang, G. (2019b). A thermodynamic constitutive model with  
1227 temperature effect based on particle rearrangement for geomaterials. *Mechanics of*  
1228 *Materials*, 139, 103180. <https://doi.org/10.1016/j.mechmat.2019.103180>
- 1229 Bai, B., Zhou, R., Cai, G., Hu, W., & Yang, G. (2021). Coupled thermo-hydro-mechanical  
1230 mechanism in view of the soil particle rearrangement of granular thermodynamics.  
1231 *Computers and Geotechnics*, 137, 104272.  
1232 <https://doi.org/10.1016/j.compgeo.2021.104272>
- 1233 Baldi, G., Hueckel, T., Peano, A., & Pellegrini, R. (1991). *Developments in modelling of*  
1234 *thermo-hydro-geomechanical behaviour of Boom clay and clay-based buffer materials*  
1235 *(Volume 1)*. [https://inis.iaea.org/search/search.aspx?orig\\_q=RN:23030425](https://inis.iaea.org/search/search.aspx?orig_q=RN:23030425)
- 1236 Baldi, G., Hueckel, T., & Pellegrini, R. (1988). Thermal volume changes of the mineral–  
1237 water system in low-porosity clay soils. *Canadian Geotechnical Journal*, 25(4), 807–  
1238 825.

- 1239 Barry-Macaulay, D., Bouazza, A., & Singh, R. M. (2011). Study of thermal properties of a  
1240 basaltic clay. In *Geo-frontiers 2011: Advances in Geotechnical Engineering* (pp. 480–  
1241 487).
- 1242 Bozis, D., Papakostas, K., & Kyriakis, N. (2011). On the evaluation of design parameters  
1243 effects on the heat transfer efficiency of energy piles. *Energy and Buildings*, 43(4),  
1244 1020–1029.
- 1245 Brandon, T. L., & Mitchell, J. K. (1989). Factors influencing thermal resistivity of sands.  
1246 *Journal of Geotechnical Engineering*, 115(12), 1683–1698.
- 1247 Burghignoli, A., Desideri, A., & Miliziano, S. (2000). A laboratory study on the  
1248 thermomechanical behaviour of clayey soils. *Canadian Geotechnical Journal*, 37(4),  
1249 764–780.
- 1250 Campanella, R. G., & Mitchell, J. K. (1968). Influence of temperature variations on soil  
1251 behavior. *Journal of the Soil Mechanics and Foundations Division*, 94(3), 709–734.
- 1252 Casarella, A., Pedrotti, M., Tarantino, A., & Di Donna, A. (2021). A critical review of the  
1253 effect of temperature on clay inter-particle forces and its effect on macroscopic thermal  
1254 behaviour of clay. *International Conference of the International Association for*  
1255 *Computer Methods and Advances in Geomechanics*, 608–615.
- 1256 Cekerevac, C., & Laloui, L. (2004). Experimental study of thermal effects on the mechanical  
1257 behaviour of a clay. *International Journal for Numerical and Analytical Methods in*  
1258 *Geomechanics*, 28(3), 209–228.
- 1259 Cheng, W., Hong, P.-Y., Pereira, J.-M., Cui, Y.-J., Tang, A. M., & Chen, R.-P. (2020).  
1260 Thermo-elasto-plastic modeling of saturated clays under undrained conditions.  
1261 *Computers and Geotechnics*, 125, 103688.
- 1262 Cho, W. J., Lee, J. O., & Chun, K. S. (1999). The temperature effects on hydraulic  
1263 conductivity of compacted bentonite. *Applied Clay Science*, 14(1–3), 47–58.

- 1264 Coccia, C. J. R., & McCartney, J. S. (2012). A thermo-hydro-mechanical true triaxial cell for  
1265 evaluation of the impact of anisotropy on thermally induced volume changes in soils.  
1266 *Geotechnical Testing Journal*, 35(2), 227–237.
- 1267 Coccia, C. J. R., & McCartney, J. S. (2016a). Thermal volume change of poorly draining  
1268 soils I: Critical assessment of volume change mechanisms. *Computers and Geotechnics*,  
1269 80, 26–40.
- 1270 Coccia, C. J. R., & McCartney, J. S. (2016b). Thermal volume change of poorly draining  
1271 soils II: model development and experimental validation. *Computers and Geotechnics*,  
1272 80, 16–25.
- 1273 Cui, Y.-J., Tang, A.-M., Qian, L.-X., Ye, W.-M., & Chen, B. (2011). Thermal-mechanical  
1274 behavior of compacted GMZ Bentonite. *Soils and Foundations*, 51(6), 1065–1074.
- 1275 Cui, Y. J., Sultan, N., & Delage, P. (2000). A thermomechanical model for saturated clays.  
1276 *Canadian Geotechnical Journal*, 37(3), 607–620.
- 1277 De Moel, M., Bach, P. M., Bouazza, A., Singh, R. M., & Sun, J. O. (2010). Technological  
1278 advances and applications of geothermal energy pile foundations and their feasibility in  
1279 Australia. *Renewable and Sustainable Energy Reviews*, 14(9), 2683–2696.
- 1280 Delage, P., Sultan, N., & Cui, Y. J. (2000). On the thermal consolidation of Boom clay.  
1281 *Canadian Geotechnical Journal*, 37(2), 343–354.
- 1282 Demars, K. R., & Charles, R. D. (1982). Soil volume changes induced by temperature  
1283 cycling. *Canadian Geotechnical Journal*, 19(2), 188–194.
- 1284 Di Donna, A., & Laloui, L. (2015). Response of soil subjected to thermal cyclic loading:  
1285 experimental and constitutive study. *Engineering Geology*, 190, 65–76.
- 1286 Di, P., Chang, D. P. Y., & Dwyer, H. A. (2000). Heat and mass transfer during microwave  
1287 steam treatment of contaminated soils. *Journal of Environmental Engineering*, 126(12),  
1288 1108–1115.

1289 ESRIG, M. I. (1969). Some temperature effects on soil compressibility and pore water  
1290 pressure. *Special Report, 103*, 231.

1291 Favero, V., Ferrari, A., & Laloui, L. (2016). Thermo-mechanical volume change behaviour of  
1292 Opalinus Clay. *International Journal of Rock Mechanics and Mining Sciences, 90*, 15–  
1293 25.

1294 Fox, P. J., & Edil, T. B. (1996). Effects of stress and temperature on secondary compression  
1295 of peat. *Canadian Geotechnical Journal, 33*(3), 405–415.

1296 François, B., & Laloui, L. (2008). ACMEG- TS: A constitutive model for unsaturated soils  
1297 under non- isothermal conditions. *International Journal for Numerical and Analytical*  
1298 *Methods in Geomechanics, 32*(16), 1955–1988.

1299 Gangadhara Rao, M., & Singh, D. N. (1999). A generalized relationship to estimate thermal  
1300 resistivity of soils. *Canadian Geotechnical Journal, 36*(4), 767–773.

1301 Ghaaowd, I., Takai, A., Katsumi, T., & McCartney, J. S. (2015). Pore water pressure  
1302 prediction for undrained heating of soils. *Environmental Geotechnics, 4*(2), 70–78.

1303 Ghahremannejad, B. (2003). *Thermo-mechanical behaviour of two reconstituted clays*.

1304 Golchin, A., Vardon, P. J., & Hicks, M. A. (2022a). A thermo-mechanical constitutive model  
1305 for fine-grained soils based on thermodynamics. *International Journal of Engineering*  
1306 *Science, 174*, 103579.

1307 Golchin, A., Vardon, P. J., & Hicks, M. A. (2022b). A thermodynamically consistent two  
1308 surface/bubble thermo-mechanical model considering thermal and mechanical cyclic  
1309 behaviour of fine-grained soils. *International Journal of Solids and Structures, 254–255*,  
1310 111847. <https://doi.org/10.1016/j.ijsolstr.2022.111847>

1311 Graham, J., Tanaka, N., Crilly, T., & Alfaro, M. (2001). Modified Cam-Clay modelling of  
1312 temperature effects in clays. *Canadian Geotechnical Journal, 38*(3), 608–621.

1313 Hillel, D. (2013). *Fundamentals of soil physics*. Academic press.

- 1314 Hong, P. Y., Pereira, J.-M., Cui, Y.-J., & Tang, A. M. (2016). A two- surface  
1315 thermomechanical model for saturated clays. *International Journal for Numerical and*  
1316 *Analytical Methods in Geomechanics*, 40(7), 1059–1080.
- 1317 Hong, P. Y., Pereira, J.-M., Tang, A. M., & Cui, Y.-J. (2013). On some advanced  
1318 thermo- mechanical models for saturated clays. *International Journal for Numerical*  
1319 *and Analytical Methods in Geomechanics*, 37(17), 2952–2971.
- 1320 Hoseinimighani, H., & Szendefy, J. (2022). A Review on Mechanisms of Thermally Induced  
1321 Volume Changes in Fine Soil. *Minerals*, 12(5), 572.
- 1322 Houston, S. L., Houston, W. N., & Williams, N. D. (1985). Thermo-mechanical behavior of  
1323 seafloor sediments. *Journal of Geotechnical Engineering*, 111(11), 1249–1263.
- 1324 Hueckel, T. A. (1992). Water–mineral interaction in hygromechanics of clays exposed to  
1325 environmental loads: a mixture-theory approach. *Canadian Geotechnical Journal*, 29(6),  
1326 1071–1086.
- 1327 Hueckel, T., & Baldi, G. (1990). Thermoplasticity of saturated clays: experimental  
1328 constitutive study. *Journal of Geotechnical Engineering*, 116(12), 1778–1796.
- 1329 Hueckel, T., & Borsetto, M. (1990). Thermoplasticity of saturated soils and shales:  
1330 constitutive equations. *Journal of Geotechnical Engineering*, 116(12), 1765–1777.
- 1331 Hueckel, T., & Pellegrini, R. (1992). Effective stress and water pressure in saturated clays  
1332 during heating–cooling cycles. *Canadian Geotechnical Journal*, 29(6), 1095–1102.
- 1333 Iwata, S., Tabuchi, T., & Warkentin, B. P. (2020). *Soil-water interactions: Mechanisms and*  
1334 *applications*. CRC Press.
- 1335 Jarad, N., Cuisinier, O., & Masrouri, F. (2019). Effect of temperature and strain rate on the  
1336 consolidation behaviour of compacted clayey soils. *European Journal of Environmental*  
1337 *and Civil Engineering*, 23(7), 789–806.
- 1338 Kadali, S., Lekshmi, S., Sharma, S., & Singh, D. N. (2013). Investigations to establish the

- 1339 influence of the thermal energy field on soil properties. *Acta Geotechnica Slovenica*,  
1340 *10(2)*, 59–76.
- 1341 Kemper, W. D., Maasland, D. E. L., & Porter, L. K. (1964). Mobility of water adjacent to  
1342 mineral surfaces. *Soil Science Society of America Journal*, *28(2)*, 164–167.
- 1343 Krishnaiah, S., & Singh, D. N. (2004a). A device for determination of thermal properties of  
1344 soil. *Journal of Testing and Evaluation*, *32(2)*, 114–119.
- 1345 Krishnaiah, S., & Singh, D. N. (2004b). Centrifuge modelling of heat migration in soils.  
1346 *International Journal of Physical Modelling in Geotechnics*, *4(3)*, 39–47.
- 1347 Kuntiwattanakul, P., Towhata, I., Ohishi, K., & Seko, I. (1995). Temperature effects on  
1348 undrained shear characteristics of clay. *Soils and Foundations*, *35(1)*, 147–162.
- 1349 Kutler, B. L., & Sathialingam, N. (1992). Elastic-viscoplastic modelling of the rate-dependent  
1350 behaviour of clays. *Géotechnique*, *42(3)*, 427–441.
- 1351 Laguros, J. G. (1969). Effect of temperature on some engineering properties of clay soils.  
1352 *Highway Research Board Special Report*, *103*.
- 1353 Laloui, L., & Cekerevac, C. (2003). Thermo-plasticity of clays: an isotropic yield  
1354 mechanism. *Computers and Geotechnics*, *30(8)*, 649–660.
- 1355 Laloui, L., & François, B. (2009). ACMEG-T: soil thermoplasticity model. *Journal of*  
1356 *Engineering Mechanics*, *135(9)*, 932–944.
- 1357 Laloui, L., Leroueil, S., & Chalindar, S. (2008). Modelling the combined effect of strain rate  
1358 and temperature on one-dimensional compression of soils. *Canadian Geotechnical*  
1359 *Journal*, *45(12)*, 1765–1777.
- 1360 Lee, J., Kim, J.-T., Chung, I.-M., & Kim, N. W. (2010). Analytical solution for heat and  
1361 moisture diffusion in layered materials. *Canadian Geotechnical Journal*, *47(6)*, 595–  
1362 608.
- 1363 Li, Y., Dijkstra, J., & Karstunen, M. (2018). Thermomechanical creep in sensitive clays.

- 1364 *Journal of Geotechnical and Geoenvironmental Engineering*, 144(11), 4018085.
- 1365 Lingnau, B. E., Graham, J., Yarechewski, D., Tanaka, N., & Gray, M. N. (1996). Effects of  
1366 temperature on strength and compressibility of sand-bentonite buffer. *Engineering*  
1367 *Geology*, 41(1–4), 103–115.
- 1368 Liu, E., & Lai, Y. (2020). Thermo-poromechanics-based viscoplastic damage constitutive  
1369 model for saturated frozen soil. *International Journal of Plasticity*, 128, 102683.  
1370 <https://doi.org/10.1016/j.ijplas.2020.102683>
- 1371 Loria, A. F. R., & Coulibaly, J. B. (2021). Thermally induced deformation of soils: A critical  
1372 overview of phenomena, challenges and opportunities. *Geomechanics for Energy and*  
1373 *the Environment*, 25, 100193.
- 1374 Ma, C., & Hueckel, T. (1993). Thermomechanical effects on adsorbed water in clays around  
1375 a heat source. *International Journal for Numerical and Analytical Methods in*  
1376 *Geomechanics*, 17(3), 175–196.
- 1377 Ma, Q. J., Ng, C. W. W., Mašín, D., & Zhou, C. (2017). An approach for modelling volume  
1378 change of fine-grained soil subjected to thermal cycles. *Canadian Geotechnical Journal*,  
1379 54(6), 896–901.
- 1380 Maghsoodi, S., Cuisinier, O., & Masrouri, F. (2020). Thermal effects on mechanical  
1381 behaviour of soil–structure interface. *Canadian Geotechnical Journal*, 57(1), 32–47.
- 1382 Maghsoodi, S., Cuisinier, O., & Masrouri, F. (2021). Non-isothermal soil-structure interface  
1383 model based on critical state theory. *Acta Geotechnica*, 1–21.
- 1384 Manthena, K. C., & Singh, D. N. (2001). Measuring soil thermal resistivity in a geotechnical  
1385 centrifuge. *International Journal of Physical Modelling in Geotechnics*, 1(4), 29–34.
- 1386 Mašín, D., & Khalili, N. (2012). A thermo- mechanical model for variably saturated soils  
1387 based on hypoplasticity. *International Journal for Numerical and Analytical Methods in*  
1388 *Geomechanics*, 36(12), 1461–1485.

- 1389 McCartney, J. S., Jafari, N. H., Hueckel, T., Sánchez, M., & Vahedifard, F. (2019). Emerging  
1390 thermal issues in geotechnical engineering. In *Geotechnical fundamentals for addressing*  
1391 *new world challenges* (pp. 275–317). Springer.
- 1392 McKinstry, H. A. (1965). Thermal expansion of clay minerals. *American Mineralogist:*  
1393 *Journal of Earth and Planetary Materials*, 50(1–2), 212–222.
- 1394 Mitchell, J. K., & Soga, K. (2005). *Fundamentals of soil behavior* (Vol. 3). John Wiley &  
1395 Sons New York.
- 1396 Mohajerani, M., Delage, P., Sulem, J., Monfared, M., Tang, A. M., & Gatmiri, B. (2012). A  
1397 laboratory investigation of thermally induced pore pressures in the Callovo-Oxfordian  
1398 claystone. *International Journal of Rock Mechanics and Mining Sciences*, 52, 112–121.
- 1399 Mon, E. E., Hamamoto, S., Kawamoto, K., Komatsu, T., & Møldrup, P. (2014). Temperature  
1400 effects on geotechnical properties of kaolin clay: simultaneous measurements of  
1401 consolidation characteristics, shear stiffness, and permeability using a modified  
1402 oedometer. *GSTF Journal of Geological Sciences (JGS)*, 1(1).
- 1403 Morin, R., & Silva, A. J. (1984). The effects of high pressure and high temperature on some  
1404 physical properties of ocean sediments. *Journal of Geophysical Research: Solid Earth*,  
1405 89(B1), 511–526.
- 1406 Mu, Q., Ng, C. W., Zhou, C., & Zhou, G. G. (2019). Effects of clay content on the volumetric  
1407 behavior of loess under heating-cooling cycles. *Journal of Zhejiang University-*  
1408 *SCIENCE A*, 20(12), 979–990.
- 1409 Naidu, A. D., & Singh, D. N. (2004). Field probe for measuring thermal resistivity of soils.  
1410 *Journal of Geotechnical and Geoenvironmental Engineering*, 130(2), 213–216.
- 1411 Ogawa, A., Takai, A., Shimizu, T., & Katsumi, T. (2020). Effects of temperature on  
1412 consolidation and consistency of clayey soils. *E3S Web of Conferences*, 205, 9010.
- 1413 Ojovan, M. I., Lee, W. E., & Kalmykov, S. N. (2019). *An introduction to nuclear waste*



- 1414           *immobilisation*. Elsevier.
- 1415 Paaswell, R. E. (1967). Temperature effects on clay soil consolidation. *Journal of the Soil*  
1416           *Mechanics and Foundations Division*, 93(3), 9–22.
- 1417 Padmakumar, G. P. (2013). *Laboratory investigations on heat migration through soil mass*.  
1418           Doctoral thesis, Indian Institute of Technology Bombay, Bombay, India.
- 1419 Pedrotti, M., & Tarantino, A. (2018). An experimental investigation into the micromechanics  
1420           of non-active clays. *Géotechnique*, 68(8), 666–683.
- 1421 Pusch, R., Karnland, O., & Hökmark, H. (1991). The nature of expanding clays as  
1422           exemplified by the multifaced smectite mineral montmorillonite. *Workshop on Stress*  
1423           *Partitioning in Engineering Clay Barriers*.
- 1424 Robinet, J.-C., Rahbaoui, A., Plas, F., & Lebon, P. (1996). A constitutive thermomechanical  
1425           model for saturated clays. *Engineering Geology*, 41(1–4), 145–169.
- 1426 Romero, E., Villar, M. V., & Lloret, A. (2005). Thermo-hydro-mechanical behaviour of two  
1427           heavily overconsolidated clays. *Engineering Geology*, 81(3), 255–268.
- 1428 Salager, S., Francois, B., El Youssoufi, M. S., Laloui, L., & Saix, C. (2008). Experimental  
1429           investigations of temperature and suction effects on compressibility and pre-  
1430           consolidation pressure of a sandy silt. *Soils and Foundations*, 48(4), 453–466.
- 1431 Schiffmann, R. L. (1971). A thermoelastic theory of consolidation. *Environmental and*  
1432           *Geophysical Heat Transfer*.
- 1433 Sherif, M. A., & Burrous, C. M. (1969). Temperature effects on the unconfined shear strength  
1434           of saturated, cohesive soil. *Effects of Temperature and Heat on Engineering Behavior of*  
1435           *Soils, Special Report*, 103, 267–272.
- 1436 Shetty, R., Singh, D. N., & Ferrari, A. (2019). Volume change characteristics of fine-grained  
1437           soils due to sequential thermo-mechanical stresses. *Engineering Geology*, 253, 47–54.
- 1438 Skipper, N. T., Refson, K., & McConnell, J. D. C. (1991). Computer simulation of interlayer

- 1439 water in 2: 1 clays. *The Journal of Chemical Physics*, 94(11), 7434–7445.
- 1440 Sreedeeep, S., Reshma, A. C., & Singh, D. N. (2005). Generalized relationship for determining  
1441 soil electrical resistivity from its thermal resistivity. *Experimental Thermal and Fluid  
1442 Science*, 29(2), 217–226.
- 1443 Stępkowska, E. T. (1990). Aspects of the clay/electrolyte/water system with special  
1444 reference to the geotechnical properties of clays. *Engineering Geology*, 28(3–4), 249–  
1445 267.
- 1446 Sultan, N., Delage, P., & Cui, Y. J. (2002). Temperature effects on the volume change  
1447 behaviour of Boom clay. *Engineering Geology*, 64(2–3), 135–145.
- 1448 Tang, A.-M., Cui, Y.-J., & Barnel, N. (2008). Thermo-mechanical behaviour of a compacted  
1449 swelling clay. *Géotechnique*, 58(1), 45–54.
- 1450 Tarantino, A., Casarella, A., Pedrotti, M., Donna, A. Di, Pagano, A., Carvalho Faria Lima  
1451 Lopes, B. de, & Magnanimo, V. (2021). Clay Micromechanics: an analysis of  
1452 elementary mechanisms of clay particle interactions to gain insight into compression  
1453 behaviour of clay. *International Conference of the International Association for  
1454 Computer Methods and Advances in Geomechanics*, 183–201.
- 1455 Towhata, I., Kuntiwattanaku, P., Seko, I., & Ohishi, K. (1993). Volume change of clays  
1456 induced by heating as observed in consolidation tests. *Soils and Foundations*, 33(4),  
1457 170–183.
- 1458 Uchaipichat, A., & Khalili, N. (2009). Experimental investigation of thermo-hydro-  
1459 mechanical behaviour of an unsaturated silt. *Géotechnique*, 59(4), 339–353.
- 1460 Vega, A., & McCartney, J. S. (2014). Cyclic heating effects on thermal volume change of  
1461 silt. *Environmental Geotechnics*, 2(5), 257–268.
- 1462 Viridi, S. P. S., & Keedwell, M. J. (1988). Some observed effects of temperature variation on  
1463 soil behaviour. *International Conference on Rheology and Soil Mechanics*, 336–354.

- 1464 von Terzaghi, K. (1923). Die Berechnung der Durchlässigkeitsziffer des Tones aus dem  
1465 Verlauf der hydrodynamischen Spannungserscheinungen. *Sitzungsber. Akad. Wiss.*  
1466 *Math. Naturwiss. Kl. Abt. 2A, 132*, 105–124.
- 1467 Wang, S., Vienna, L. S., Wu, W., Vienna, L. S., Zhang, D., & Kim, J. (2020). *Thermal-*  
1468 *mechanical Behaviour of Saturated Soil : A Review Study SOIL MECHANICS AND.*  
1469 *May*.
- 1470 Yao, Y.-P., & Zhou, A. N. (2013). Non-isothermal unified hardening model: a thermo-elasto-  
1471 plastic model for clays. *Géotechnique, 63*(15), 1328–1345.
- 1472 Yavari, N., Tang, A. M., Pereira, J.-M., & Hassen, G. (2016). Effect of temperature on the  
1473 shear strength of soils and the soil–structure interface. *Canadian Geotechnical Journal,*  
1474 *53*(7), 1186–1194.
- 1475 Ye, W.-M., Wan, M., Chen, B., Chen, Y.-G., Cui, Y.-J., & Wang, J. (2012). Temperature  
1476 effects on the unsaturated permeability of the densely compacted GMZ01 bentonite  
1477 under confined conditions. *Engineering Geology, 126*, 1–7.
- 1478 Yin, Z.-Y., Zhu, Q.-Y., & Zhang, D.-M. (2017). Comparison of two creep degradation  
1479 modeling approaches for soft structured soils. *Acta Geotechnica, 12*(6), 1395–1413.
- 1480 Yong, R. N. (1999). Overview of modeling of clay microstructure and interactions for  
1481 prediction of waste isolation barrier performance. *Engineering Geology, 54*(1–2), 83–91.
- 1482 Zhang, Z. (2017). A thermodynamics-based theory for the thermo-poro-mechanical modeling  
1483 of saturated clay. *International Journal of Plasticity, 92*, 164–185.
- 1484 Zhang, Z., & Cheng, X. (2017). A fully coupled THM model based on a non- equilibrium  
1485 thermodynamic approach and its application. *International Journal for Numerical and*  
1486 *Analytical Methods in Geomechanics, 41*(4), 527–554.
- 1487 Zhou, C., Fong, K. Y., & Ng, C. W. W. (2017). A new bounding surface model for thermal  
1488 cyclic behaviour. *International Journal for Numerical and Analytical Methods in*

- 1489            *Geomechanics*, 41(16), 1656–1666.
- 1490    Zhu, Q.-Y., & Qi, P. (2018). Numerical Modeling of Thermal-Dependent Creep Behavior of  
1491            Soft Clays under One-Dimensional Condition. *Advances in Civil Engineering*, 2018.
- 1492    Zhu, Q.-Y., Yin, Z.-Y., Zhang, D.-M., & Huang, H.-W. (2017). Numerical modeling of creep  
1493            degradation of natural soft clays under one-dimensional condition. *KSCE Journal of*  
1494            *Civil Engineering*, 21(5), 1668–1678.
- 1495    Zhu, Q.-Y., Zhuang, P.-Z., Yin, Z.-Y., & Yu, H.-S. (2021). State parameter–based  
1496            thermomechanical constitutive model for saturated fine-grained soils. *Canadian*  
1497            *Geotechnical Journal*, 58(7), 1045–1058.
- 1498